Biological Effects of Ionizing Radiation

10

Abstract In this chapter, the biological effects of ionizing radiation are presented, beginning with the radiobiology of the mammalian cell. This includes the chromosome and chromatid aberrations resulting from radiation-induced damage of DNA (primarily double-strand breaks, DSBs), the mechanisms, and categories of cell death and of germ-cell mutation. The models of various cell survival curves are described, culminating with the linear-quadratic (LQ) model. The effects of ambient oxygen and LET upon producing cell lethality are considered. Due to its clinical applications, including therapeutic nuclear medicine, the LQ model is studied in detail. The LQ model is derived from a model of DSB production and repair kinetics and the Lea–Catcheside dose-protraction factor and the biological equivalent dose are derived from this result. Human somatic effects of radiation, including epidemiological studies of irradiated populations which provide our estimates of radiation risk, are reviewed. The chapter concludes with consideration of the radiation protection of the nuclear medicine patient, which includes the derivation of the effective dose, and a brief introduction to radiobiology considerations in therapeutic nuclear medicine.

Contents

B.J. McParland, *Nuclear Medicine Radiation Dosimetry*,
DOI 10.1007/978-1-84882-126-2_10,

10.1 Introduction

Up to this point, only the physical effects resulting from exposure to ionizing radiation have been considered. The intents of these discussions were the ability to, first, calculate the radiation fluence in a medium and, second, calculate the resulting energy transfer and absorbed dose to that medium. The concept of a medium in the context of medical radiation dosimetry is more complex than has been considered as the medium is now a living organ or tissue which responds biologically to the energy deposited by radiation.

The division of nuclear medicine into diagnostic and therapeutic applications is a result of different considerations of the biological effects of ionizing radiation (BEIR). Diagnostic nuclear medicine seeks to avoid all biological effects by limiting the absorbed dose to a minimally-acceptable level, but whilst still maintaining the diagnostic efficacy of the study. As a result, the biological responses to these low absorbed doses are probabilistic and limited to oncogenesis and hereditary effects. Therapeutic nuclear medicine seeks neoplastic cell death subject to the optimization of minimizing the radiotoxicity that uninvolved healthy tissues can be subjected to. Despite the differing biological endpoints of interest to diagnostic and therapeutic nuclear medicine, a common understanding of cellular response to ionizing radiation is required for both. The challenges of such understanding are profound. In diagnostic nuclear medicine, one focuses on radiation-induced mutagenesis where ionizing radiation can, in the first case of a somatic cell, result in the production of a malignant cell. This transformation is the result of four or more genetic modifications:

- Overexpression of viral genes or proto-oncogenes
- Loss of apoptosis genes
- Mutations of tumor-suppressing genes (e.g., p53)
- Mutations of those genes necessary for DNA repair

In addition to these effects upon somatic cells are those inflicted upon germ cells. These effects will be, at low absorbed doses, the induction of mutations that can be expressed as inherited genetic effects manifested in the progeny. Despite popular folklore, the characteristics of these mutations are no different than those that occur naturally. Ionizing radiation can only increase the frequency of presentation of these otherwise naturally and spontaneously occurring mutations. At higher absorbed doses, the radiation-induced deaths of spermatogonia can lead to either temporary or permanent sterility in the male depending upon the magnitude of the absorbed dose conferred; in the female, temporary sterility is unachievable and death of the oocytes results in permanent sterility.

In therapeutic nuclear medicine, one seeks the optimization of the probabilities of tumor control and normal tissue complication (radiotoxicity). Tumor control is optimized through the selection of the appropriate vector to transport the radionuclide to the target cells (specificity), the physical half-life of the radioisotope so as to impede the ability for tumor cells to repair radiation damage and the appropriate isotope in terms of its radiation decay scheme. The large mean-free path of photons precludes photon emitters as radiotherapeutics and so interest is in those isotopes that emit charged particulate radiations: α or β particles or the very short-range Auger/Coster–Kronig electrons emitted following electron capture or internal conversion decays.

Consider the radiobiology of diagnostic nuclear medicine. One seeks the minimization, or perhaps even mitigation, of biological effects resulting from the exposure to low absorbed doses of radiation. The fundamental radiobiology of the mammalian cell is a foundation for estimating or modeling the subsequent risks presented to the patient. While knowledge of the response of the individual cell to radiation is required in order to mathematically model these risks, it is not sufficient. Epidemiological data derived from the consequences of populations exposed to ionizing radiation (deliberate or otherwise) are essential to deriving these risk estimates. In most cases, the absorbed doses received by such cohorts are much higher than those received by the medical imaging patient. Hence, it is necessary to extrapolate the observed risk, such as increased cancer incidence or mortality, at these higher absorbed doses to the lower doses more reflective of the diagnostic case. The extrapolation models used will rely greatly upon concepts derived from cellular radiobiology.

On the other hand, therapeutic nuclear medicine considerations have been historically much less reliant upon mathematical modeling and are often based purely upon clinical experience of radiotoxicity limitations. Administered activities of therapeutic radionuclides are still, generally, crudely applied in terms of a single value (MBq) or otherwise normalized to patient body surface area (MBq/m^2) or body weight (MBq/kg). Such approaches – which would not even be contemplated in the modern-day prescription of external beam radiotherapy absorbed doses – are being supplanted by more patient-specific prescriptions. Pretherapy imaging of the therapeutic moiety (at either a diagnostic level of activity if it should emit photons or of its replacement with a photon-emitting isotope, e.g., the replacement of ^{131}I with ^{123}I) allows an estimation of the uptake of the therapeutic agent in the region of interest. This can then be used to derive the amount of therapeutic activity required to obtain the absorbed dose and biological effect desired.

10.2 Radiobiology of the Mammalian Cell

10.2.1 Introduction

All biological processes in a unicellular organism such as a bacterium occur within that single cell. In multicellular organisms (metazoa), specific cell groups "specialize" in conducting distinct functions. As a result, the differential magnitudes of such specializations can frequently make it difficult to define a typical cell representative of all of those in the body. However, there is a significant degree of common internal structure (organelles) among cells that allow a general specification to be made.

Metazoans are defined as multicellular eukaryotic organisms. This chapter is concerned exclusively with mammalian cells. The first obvious reason for this distinction is that we are ultimately interested in the response of human tissues to ionizing radiation. The second, and subtle, reason is that nonmammalian cells exhibit markedly different responses to ionizing radiation than do mammalian cells due to the much higher deoxyribonucleic acid (DNA) content of the latter.

10.2.2 Structure of the Mammalian Cell

10.2.2.1 Cellular Structure

Despite their differentiation in terms of function, all mammalian cells have certain common attributes. With the exception of the erythrocyte, all contain subcellular structures known as organelles and are eukaryotic, i.e., have a nucleus containing DNA. The exceptional erythrocyte (red blood cell) contains a nucleus at its early stage of development, but extrudes it (along with other organelles) during maturation in order to increase the amount of hemoglobin content it may carry.

The intracellular matrix, or cytoplasm, contains the nucleus and other organelles. These organelles are:

Mitochondria: Ellipsoid-shaped structures responsible for energy production within the cell

Golgi apparatus: Responsible for the storage and transportation of secretory products to the external environment

Endoplasmic reticulum: A network of tubules and cisternae responsible for the folding and transportation of proteins to the cell membrane

Ribosomes: Spherical structures which are the site of protein synthesis and are either free in the cytoplasm or connected to the endoplasmic reticulum

Lysosomes: Contain enzymes responsible for the digestion of vacuoles formed by the phagocytosis of solid material (e.g., foreign bacteria) and for the eradication of worn-out organelles

Centrioles: Paired cylindrical structures involved in cell division (cytokinesis). During this stage, they move to opposite ends of the nucleus and form the ends of the mitotic spindle (bundles of microtubules of protein filaments)

10.2.2.2 Types of Mammalian Cells

Despite the commonality of a nucleus and organelles, mammalian cells differ markedly in terms of morphology, function and cell kinetic properties, and radiosensitivity. The four primary categories of tissues formed by mammalian cells are:

Connective: Fibrous tissue which holds organs in place and forms ligaments and tendons. It is subdivided further into categories of loose, dense, elastic, adipose, and reticular connective tissues.

Epithelial: Tissue consisting of cells lining cavities and lumen and organ surfaces. This tissue forms the skin and lines, for example, the gastrointestinal (GI) tract and glandular ducts.

Nervous: Tissue made up of neurons, which transmit electrical impulses, and the supportive neuroglia which are made up of microglia and macroglia cells.

Muscular: Contractile tissue made up of three categories – skeletal or voluntary muscle anchored by tendons to bone and which is under voluntary control; smooth or involuntary muscle found within the viscera such as the esophagus and the GI tract and the urinary bladder; and cardiac muscle which is similar to skeletal muscle although it is involuntary and is found in the heart alone.

10.2.2.3 DNA

DNA is a long polymer made up from repeating nitrogenous bases (adenine, guanine, thymine, and cytosine) and exists as an intertwined double helix with the bases binding the helices. The strand itself consists of alternating phosphate and sugar (deoxyribose) groups and has a diameter of the order of 2.5 nm. The nucleotides bind pair-wise specifically: adenine (purine) with thymine (pyrimidine) and cytosine (pyrimidine) with guanine (purine), as shown schematically in Fig. 10.1. The groupings of bases are thus complementary: adenine will bind with thymine and cytosine always binds with guanine.

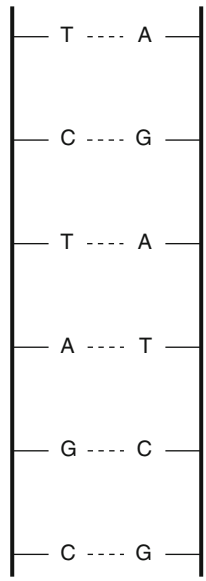

Fig. 10.1 Schematic representation of the binding between thymine (*T*)-adenine (*A*) bases and cytosine (*C*)-guanine (*G*) bases

10.2.2.4 Chromatin, Chromosomes, and Chromatids

As the length of the DNA contained within the eukaryotic cell is several thousand times the dimension of the cell, it must be compressed through sequential folding in order to fit within the nucleus and yet still be accessible. This folding of DNA forms the organized packed structure chromatin, which is a thread-like entity within the nucleus made up from DNA and protein. This is further integrated into the chromosome. The name chromosome is derived from the Greek *chroma* and *soma*, or "colored body," reflecting the chromosome's ability to take histologic stain. During mitosis, it condenses to form sister chromatids, along with the centromere, a site which does not take histologic stain. Its role in cell division, or mitosis, is to be explained below.

10.2.2.5 Proliferation and Cell Cycle

A cell divides into two daughter cells following a cycle defined by sequential mitotic divisions. This cycle is partitioned into two phases of the short metaphase during which the cell undergoes mitosis and a longer interphase. Much activity goes on within the cell during the interphase so it is subdivided into three intermitotic phases: the two gap phases, G_1 and G_2, which follow and precede the mitotic phase, respectively, during which there is apparent cellular inactivity and the S DNA synthesis phase.

During the G_1 phase, the cell produces enzymes required for the S phase. The length of this is highly variable. Synthesis of DNA and replication of the chromosomes occurs during the S phase. In the G_2 phase, each chromosome is made up of two sister chromatids (Fig. 10.2).

During the mitotic (M) phase, the cell divides. This phase is made up of the prophase, prometaphase, metaphase, anaphase, and telophase (Hall and Giaccia

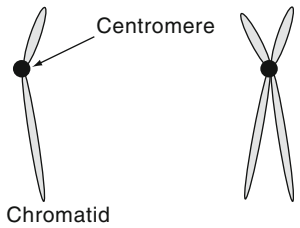

Fig. 10.2 Condensed chromosome morphology during (*left*) interphase and (*right*) the S phase of the cell cycle during which it has duplicated

2006). The subnuclear actions that occur during these mitotic phases are:

Prophase: During this phase, chromatin condenses to form the visible chromosome and ends with the maximal condensation and the disappearance of the nuclear membrane.

Prometaphase: The nuclear membrane and nucleoli having disappeared, the centrioles move to opposite sides of the nucleus and spindle fibers form between them.

Metaphase: Following the disappearance of the nuclear membrane, the cytoplasm and nuclear plasma intermix. The spindle fibers from the centrioles attach to the centromeres, the latter dividing to signal the end of metaphase.

Anaphase: The chromosomes are pulled to the opposing poles of the nucleus.

Telophase: The daughter chromosomes uncoil, the spindle fibers break off and nuclear membranes are formed around each ensemble of chromosomes and nucleoli regenerate. The chromosomes disperse into chromatin and the nucleus resumes its indistinct interphase appearance.

While the interphase of the cell cycle is that part when mitosis is not occurring, it accounts for other significant cell processes. The intermitotic phase which is experimentally most easily recognized is the S phase which, in most cases, is the only time during the cell cycle that DNA is synthesized.[1] On the other hand, RNA and protein synthesis can occur at any time throughout the interphase. Movement through the cell cycle is governed by proteins known as cyclins with "check points" at the G_1–S and G_2–M junctions. Transition through these junctions is enabled by cyclin-dependent kinases (Fig. 10.3).

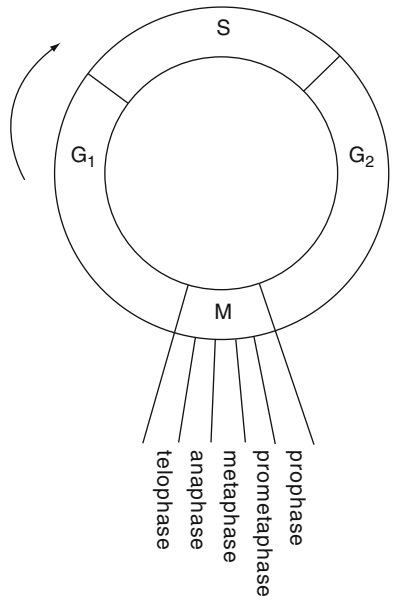

Fig. 10.3 The cell cycle where M is when mitosis occurs and the intermitotic phases (interphase) is made up of two gap phases, G_1 and G_2, and the S DNA synthesis phase. Some cells can enter a "resting" phase, G_0, following the M–G_1 junction before entering the G_1 phase. The length of the G_1 phase can be highly variable

10.2.3 Radiation-Induced Damage to the Cell

10.2.3.1 Introduction

Any discussion of cellular damage caused by ionizing radiation must begin with an understanding of what are the radiation-sensitive sites within the cell. Although mainly circumstantial, there is overwhelming evidence that the target is chromosomal DNA. That it is the cell nucleus that is sensitive to radiation and the cytoplasm insensitive has been demonstrated by two different categories of experiment. The first

[1]This statement is not strictly true as mitochondrial DNA synthesis can occur outside the S phase as can unscheduled nuclear DNA synthesis following radiation-induced damage.

uses the physical directing of ionizing radiation to the nucleus. This can be achieved by, for example, placing a needle tip, coated with an α-emitting isotope of polonium, adjacent to the nucleus (Munro 1961). Recall that such α particles have low energy and short ranges. Hence, with the appropriate selection of α-particle energy and design of the applicator, it is possible to ensure that the nucleus is the only organelle receiving an absorbed dose. Such experiments have demonstrated that the mean lethal absorbed dose to the nucleus is 1.5 Gy whereas an absorbed dose as high as 250 Gy delivered to the cytoplasm can have no effect upon cell proliferation. A similar, but more sophisticated, approach of subcellular irradiation is through a "microbeam" of charged ions bombarding subcellular targets in vitro (Folkard et al. 2007). The secondary type of experiment compares the effects upon the cell of tritiated water with those of tritiated thymidine (deoxythimidine). As thymidine is integral to DNA synthesis, labeling with tritiated thymidine will localize the short-range β particles emitted during the β decay of ^{3}H to ^{3}He directly to the DNA in the nucleus whereas the distribution of tritiated water within the cell is uniform and nonspecific throughout the cell. It is found that the radiation sensitivity of the cell to tritiated thymidine is several orders of magnitude greater than to tritiated water, implicitly suggesting that radiation damage to the nucleus is the center of cellular radiation damage.

Now that the nucleus has been established to be the most radiosensitive organelle, it is interesting to see if it is possible to delve deeper in terms of spatial resolution and identify a subnuclear structure that causes this radiosensitivity. This can be inferred by the spatial dimensions of the energy depositions of low-LET radiations, such as soft X-rays (energies below 1 keV). Recall from Chap. 7 that the energy deposition of the charged particles resulting from photon–matter interactions is stochastic, especially at small spatial dimensions, and is distributed nonuniformly along the trajectory of the particle. In the nomenclature promoted by Hall and Giaccia (2006), the energy deposition distributions are categorized here as either a "spur," which has a maximum energy deposition of 100 eV, is about 4 nm in diameter and typically contains three ion pairs, or a "blob" which has an energy deposition of between 100 and 500 eV, is about 7 nm in diameter and typically contains up to 12 ion pairs. For low-LET radiation, virtually all of the energy deposition is in the form of "spurs" and, as the spatial dimension of the spur is comparable to the 2 nm width of the DNA double helix, this provides further circumstantial evidence that nuclear DNA is the radiosensitive target.

10.2.3.2 Mechanisms of Radiation-Induced Damage

Indirect Effect

Photons and moving charged particles traversing a medium ionize atoms, leaving free electrons and ions in their wake. As the composition of the cell is about 70% water, the effects of the ionization of water by radiation (water radiolysis) will be of dominant interest,

$$H_2O \xrightarrow{\text{Radiation}} H_2O^{+\bullet} + e^-$$

where the superscripts + indicate a positive ion and • an unpaired electron. Another channel is the simple excitation of the water molecule,

$$H_2O \xrightarrow{\text{Radiation}} H_2O^{*}.$$

$H_2O^{+\bullet}$ is an ion radical[2] with a lifetime of the order of 0.1 ns and is highly reactive. The liberated electron can be subsequently hydrated, i.e., trapped by surrounding water molecules that it has polarized so as to form an aqueous electron,

$$e^- + H_2O \rightarrow (e^-)_{aq}.$$

As the electron is ejected in the ionization event with considerable energy so as to be displaced considerably from the point of ionization, the production of the $H_2O^{+\bullet}$ will not be in equilibrium and the free radical unable to recombine with the ejected electron.

[2]An atom or molecule is a free radical if it has an unpaired electron, even though it can also be electrically neutral. Free radicals are chemically reactive. An ion radical is both an ion and a free radical and, hence, is highly reactive.

The free radical can then either decompose to yield a free proton and a free neutral hydroxyl radical.

$$H_2O^{+\bullet} \rightarrow H^+ + OH^\bullet$$

Or interact with a water molecule to again form a free neutral hydroxyl radical,

$$H_2O^+ + H_2O \rightarrow H_3O^+ + OH^\bullet.$$

The aqueous electron can also interact with a water molecule to form,

$$(e^-)_{aq} + H_2O \rightarrow OH^\bullet + H^+$$

and it can interact with H^+ from other ionizations to form the hydrogen radical,

$$(e^-)_{aq} + H^+ \rightarrow H^\bullet.$$

While the above chain of reactions is, in fact, far more involved, the three most important reactive chemical species created and their relative yields per initial ionization are:

$$(e^-)_{aq}: \quad 45\%$$

$$OH^\bullet: \quad 45\%$$

$$H^\bullet: \quad 10\%.$$

Following their production, the reactive species (which have longer lifetimes of the order of 10 μs compared to the 0.1 ns lifetimes of ions) diffuse and, if the ionization is sufficiently close to the DNA double helix, can migrate to the helix and damage it. The $OH^\bullet$ is a particularly potent species in causing DNA damage as it can extract an electron from the DNA and leave behind a highly reactive site. This category of DNA damage by radiolytic products is known as the indirect effect.

It is also possible for these reactive radiolytic species to interact with each other, especially in the volume around the initial ionization event and prior to any diffusion, and neutralize. Two examples are:

$$OH^\bullet + H^\bullet \rightarrow H_2O$$

and

$$H^\bullet + H^\bullet \rightarrow H_2.$$

As a result, it is possible to modify the indirect effect, i.e., to sensitize or protect the cell from radiation effects by affecting these reactive species. Consider the dynamic equilibrium of an organic molecule ionized to form two free radicals,

$$RH \xrightarrow{\text{Radiation}} R^\bullet + H^\bullet.$$

Because of the proximity of $R^\bullet$ and $H^\bullet$ following the ionization event, there is a high probability that they will recombine immediately and, hence, cannot proceed to cause an indirect effect upon the DNA target. This interaction between $R^\bullet$ and $H^\bullet$ changes dramatically in the presence of oxygen. As oxygen is a free radical scavenger, it is possible in an oxygenated environment for the radicals to interact with the oxygen,

$$R^\bullet + H^\bullet + 2O_2 \rightarrow RO_2^\bullet + HO_2^\bullet.$$

Oxygen can thus "fix" the result of two free radicals which are then subsequently free to damage the DNA. Hence, hypoxia, which commonly occurs in tumors receiving insufficient vascularization, leads to radioresistance.

Direct Effect

Whereas the indirect effect of ionizing radiation upon DNA is through the intermediaries of radicals as a result of water radiolysis, it is also possible for DNA damage to be produced through the direct ionization of the DNA molecule by radiation.

Relative Contributions

The relative contributions of indirect and direct effects upon DNA damage are of practical importance in consideration of the above discussion regarding the use of radiation protectors or sensitizers to modify the indirect effect. It is believed that about two-thirds of the radiation-induced damage to the DNA is due to the indirect effect (Nais 1998).

10.2.3.3 Radiation-Induced DNA Lesions

Introduction

There are three categories of ionizing radiation-induced chemical changes to DNA that result in damage to the structure of the DNA.

Base Alterations

These are effects inflicted upon the purine and pyrimidine bases by ionizing radiation. Many of these insults are benign with no apparent effect postirradiation. Others result in miscoding during DNA replication leading to a mutation.

Single-Strand Breaks

A single-strand break (SSB) is the removal of one of a pair of bases through damage. Repair is possible during the DNA synthesis phase of the cell cycle as the remaining undamaged base will provide a complementary template for a base on opposing strands to form. Hence, cell lethality is not necessarily a consequence of the damage. Mutation, however, is possible if misrepair occurs or if repair is incomplete. SSBs on both strands can also be repairable if they are sufficiently separated, as shown in Fig. 10.4, as they may be considered independent breaks as such.

Double-Strand Breaks

A double-strand break (DSB) is one in which both DNA strands are broken at the same point or very close together, as shown in Fig. 10.4. DSBs are likely to be accompanied by extensive base damage and following such breaks, the chromatin splits into two segments. The production, repair, and misrepair of DSBs are of great importance to understanding radiation-induced cell lethality. The damaged chromosome may restitute (i.e., the damaged ends may reconnect) resulting in the repair of the physical integrity of the DNA chain but not reproducing the original nucleotide sequence. Binary misrepair of DSBs in two adjacent chromosomes can result in the illegitimate interaction of the two damaged chromosomes culminating in cell death. Of particular importance to the repair of cells damaged by low-LET radiation or low absorbed dose rates is that a DSB can result from two independent chromosomal lesions that occurred at different times but in close physical proximity. If the temporal separation between these two ionizations is sufficiently great, the cell is provided with the opportunity to repair the first lesion before the second, and potentially combinatorial fatal, lesion occurs.

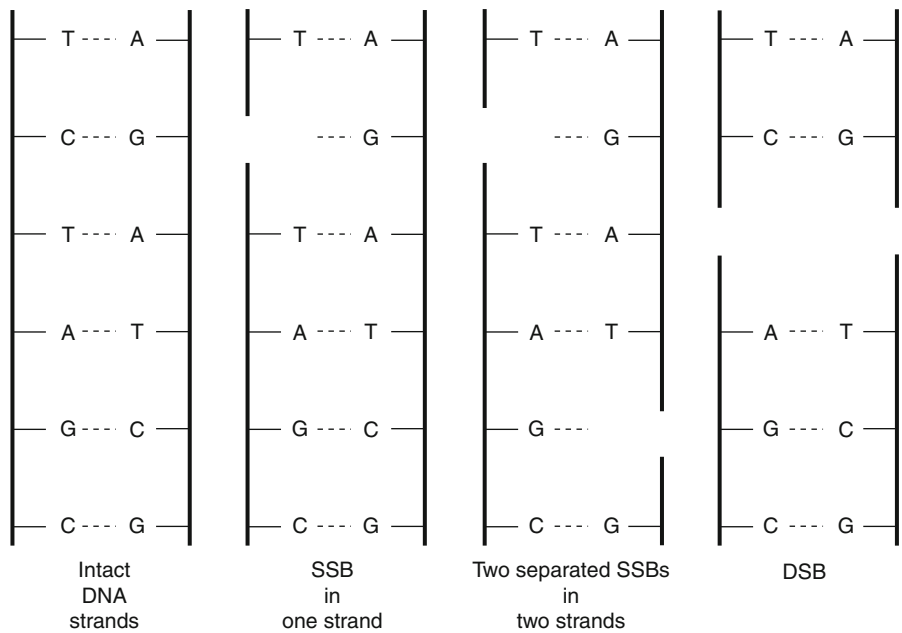

Fig. 10.4 SSB and DSB. An SSB or a pair of widely separated SSBs can be repaired using the undamaged remaining base as a template. A DSB leads the chromatin to separate into two

Summary

The probabilities of base alterations and SSBs occurring per unit dose are, as expected, greater than that of DSBs. Table 10.1 summarizes the incidences of damage per unit absorbed dose (for low-LET radiation) and the lethal consequences as the probability of cell death per lesion induction.

10.2.3.4 Chromosome and Chromatid Aberrations

Lethal

Three types of lethal chromosomal aberrations that can be induced by radiation through the interactions of a minimum of two strand breaks are considered. Further information on chromosomal aberrations can be found in Savage (1983) and in Hall and Giaccia (2006).

Table 10.1 Types of ionizing radiation-induced DNA lesions (low-LET radiation)

Lesion type	Incidence per unit absorbed dose (Gy^{-1})	Relative lethality (%)
Alteration of nucleotides	10^3	1
SSB	10^3	1
DSB	40	95

Dicentric

This type of aberration is the result of the replication of two chromosomes which were damaged in interphase with single breaks and which subsequently interacted, as shown in Fig. 10.5. Following replication during the S phase, the result is a chromosome with two centromeres and two fragments without centromeres. The latter discontinue at the subsequent mitosis as a centromere is required to move to a pole during anaphase in the M-phase of the cell cycle.

Centric Ring

A centric "ring" chromosome aberration can be the result of a DSB of a single chromosome which can recombine to form the cyclic structure shown in Fig. 10.6. The result following the S phase is a pair of overlapping ring chromosomes and a pair of acentric chromosome fragments which, as noted before, will be lost at mitosis.

Anaphase Bridge or Interarm Aberration

Whereas dicentric and ring aberrations are associated with changes to the chromosome (and are the result of presynthesis irradiation), the anaphase bridge is a chromatid aberration, as shown in Fig. 10.7, and is a result of postsynthesis irradiation during the G_2 phase. As separation of the replicated cells is impossible, this nature of aberration is fatal.

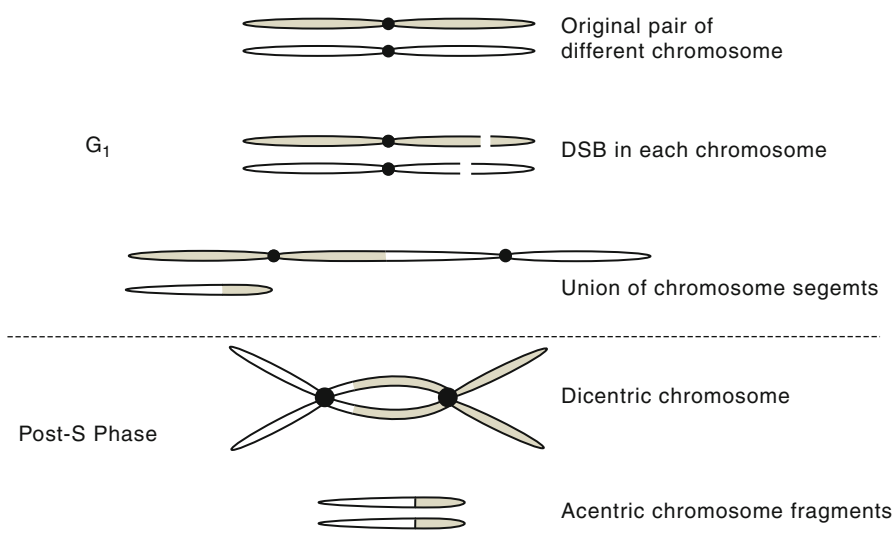

Fig. 10.5 Production of a dicentric chromosome aberration. Prior to replication, two chromosomes are "broken" by irradiation and then intercombine. Following replication, a dicentric chromosome (with two centromeres) is created in addition to two acentric chromosome fragments

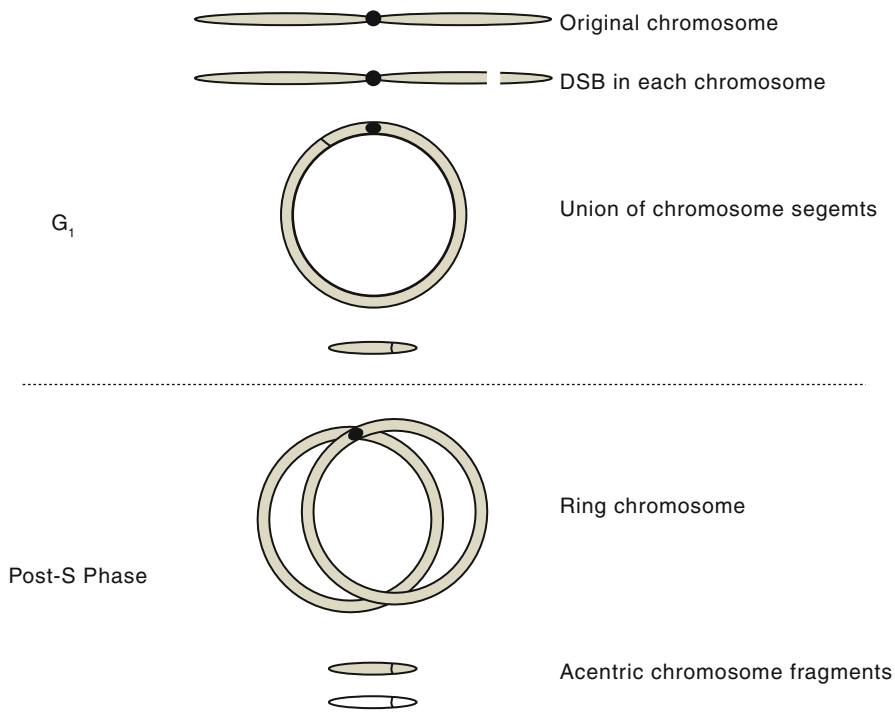

Fig. 10.6 Formation of a ring chromosome aberration. A DSB in a single chromosome is followed by a reconnection to form a ring chromosome and an acentric segment. Following replication, a pair of overlapping ring chromosomes is produced and a pair of acentric fragments which are lost at the subsequent mitosis

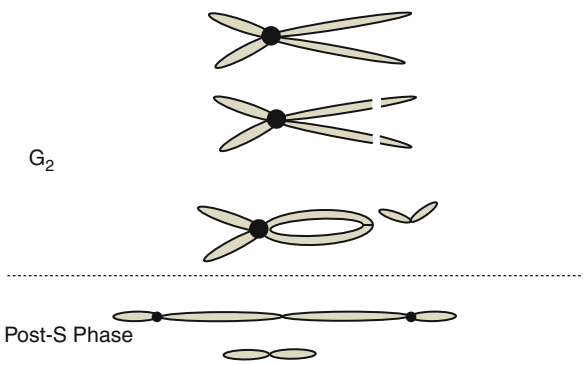

Fig. 10.7 Formation of an anaphase bridge. A chromosome in the G_2 phase is irradiated and a break occurs in both chromatids which recombine at the ends, forming an acentric chromatid fragment. Following anaphase, the centromeres will be attracted to each pole, thus stretching the chromatid between poles. The acentric chromatid segment will be lost

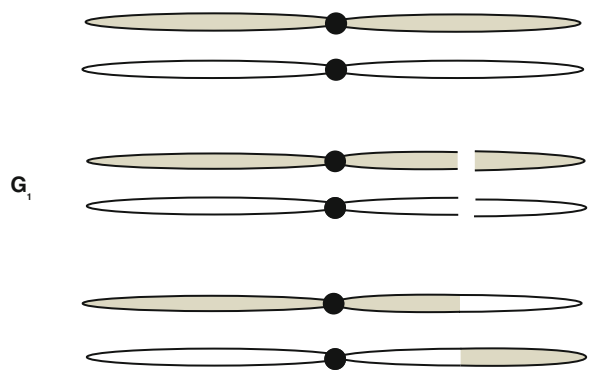

Fig. 10.8 Symmetric translocation. Following irradiation of two chromosomes in the G_1 phase, breaks are produced. The chromosome segments are exchanged between the chromosomes

Nonlethal

Symmetric Translocation

This is a not necessarily lethal chromosomal aberration resulting from the exchange of chromosome fragments formed during irradiation during the G_1 phase, as shown in Fig. 10.8. Such translocations can, however, activate an oncogene leading to a malignancy.

10.2.4 Radiation-Induced Cell Death

10.2.4.1 Introduction

The death of an irradiated cell is only one consequence of its exposure to ionizing radiation. In fact, the term "cell death" requires clarification and expansion. The most common mode of radiation-induced mammalian

cell death is that in which the cell fails to undergo further mitosis and replicate, although it may remain metabolically active. Death can also occur during interphase due to apoptosis, frequently referred to as "programmed cell death" or "cell suicide." Radiation-induced cell death can be a consequence of the peculiar "bystander effect." In this effect, an unirradiated cell in proximity to an irradiated cell dies, presumably through the effects of some toxic agent released by the irradiated cell.

10.2.4.2 Mitotic Death

This is the most frequent means of radiation-induced cell death and is the result the of lethal chromosome asymmetric-type exchange aberrations previously discussed. Cell death results when the irradiated cell attempts mitosis; this can occur not only at the first attempt at mitosis postirradiation, but also during attempts at subsequent cell divisions. Mitotic death has been quantitatively demonstrated by Cornforth and Bedford (1987). They demonstrated that the logarithm of the surviving fraction (SF) of a population of irradiated cells was exactly equal to the mean number of lethal chromosomal aberrations per cell.

While mitotic processes can be halted as consequences of irradiation, it is usually possible for cell metabolism to continue. As a result, this procession of metabolism in the undivided cell leads to an exponential growth in cell size which eventually reaches a plateau. Even though such a "giant cell" will grow, it is considered to be "dead" as it has lost its proliferative capacity.

10.2.4.3 Interphase Death and Apoptosis

Cell death can also occur from irradiation during interphase, although this requires much higher absorbed doses than those which induced mitotic death. The mean absorbed dose required for mitotic death is of the order of 1–2 Gy in a single exposure. Should a population of cells be irradiated to an absorbed dose of up to 10^3 Gy in a single exposure, cellular metabolism and function ceases and necrotic death occurs. Such an extreme ionizing radiation insult is largely irrelevant to our considerations of diagnostic and therapeutic nuclear medicine. However, interphase death can occur at lower absorbed doses. Apoptosis is a naturally-occurring means of cell death in both tumor and normal tissue. It is also present in the developing embryo where obsolete tissues no longer required in its development are eradicated. It can be triggered by ionizing radiation in specific cell types, in particular, lymphatic and hematopoietic cells, through initiation by the p53 tumor-suppressor gene. Following the induction of radiation-induced DNA damage, the amount of p53 accumulates and leads to a delay in the progress to mitosis so as to allow time for the cell to repair this damage. If repair is not possible or is unsuccessful, the p53 gene can then initiate apoptosis in order to remove the nonfunctional cell from its environment. However, should the p53 gene be inactivated through a mutation, apoptosis cannot occur and cell immortality becomes possible.

A cell entering apoptosis begins this process by isolating itself from its neighboring cells. Chromatin condenses, the cellular nucleus fragments and the cytoplasm dehydrates with the result that the cellular volume shrinks. Phagocytosis follows to eradicate the fragmented apoptotic bodies.

10.2.4.4 Bystander Effect

This is an intriguing phenomenon in which a biological response is detected in cells that have not been irradiated but which are in close physical proximity to one that has (Sgouros et al. 2007). While evidence for the effect was first seen in the 1940s and 1950s (Hall 2003; Mothersill and Seymour 2001), current interest in was ignited by the work of Nagasawa and Little (1992) showing an elevated frequency of chromosomal damage relative to that expected for absorbed doses as low as 310 μGy following 3.3 MeV α-particle irradiation from a ^{238}Pu source. Thirty percent of the cells studied demonstrated an increase in sister chromatid exchanges, even though only 1% of the cells had actually been traversed by an α particle (see, also, Kahim et al. 1992). Since then, the bystander effect has been demonstrated for X-rays and protons. As unirradiated cells have been killed following the transfer of a medium which contained irradiated cells, it is presumed that the

bystander effect is due to cytotoxins released by the irradiated cells.

10.2.4.5 Categories of Radiation-Induced Cell Damage

Introduction

The consequences following the irradiation of a cell are manifold and require specific definitions. This is necessary in order to differentiate between the results of the effects of ionizing radiation upon cells and the spectrum of normal cell variants. For example, mitotic cell death has already been described as the irradiated cell's loss of reproductive capacity caused by radiation damage. Yet, neurons do not undergo mitosis following full fetal development. Hence, the first effect of irradiation is the lack of the presentation of any damage whatsoever. While radiation-induced damage to the DNA may have occurred, it is possible that, even without repair, the DNA damage has had no impact upon the cell's ability to reproduce or upon the cell's functional ability.

When damage does occur and which can cause or lead to cell death, further differentiation of the damage is required. Clearly, the definition of lethal damage is immediately obvious. Nonlethal damage results in the retention of reproductive capacity, albeit perhaps with a reduced growth rate. The two categories of sublethal damage and potentially lethal damage are of great practical interest to radiobiology and are looked at in detail here.

Sublethal Damage

This is the category defined as the result of two independent radiation lesions. The first insult can undergo repair, but if a second radiation-induced insult is received prior to the first damage having been completely repaired, cell death results. For example, consider a DSB created in a single chromosome following irradiation. It is possible for the cell to be able to repair this damage by recombining the chromosomal fragments; the result is not necessarily lethal to the cell. However, if, before this DSB is repaired, another DSB is created in an adjacent chromosome, an illegitimate and likely lethal binary misrepair can result such as, for example, a dicentric. Thus, the first damage to have been incurred is referred to as being sublethal. The presence of sublethal damage can be demonstrated experimentally by irradiating cells in a split-dose regimen, as shown conceptually in Fig. 10.9. At low time separations between absorbed dose administrations, the probability of survival is reduced and, as the time separation between exposures increases, the SF increases to finally reach a plateau reflecting the complete repair of sublethal damage.

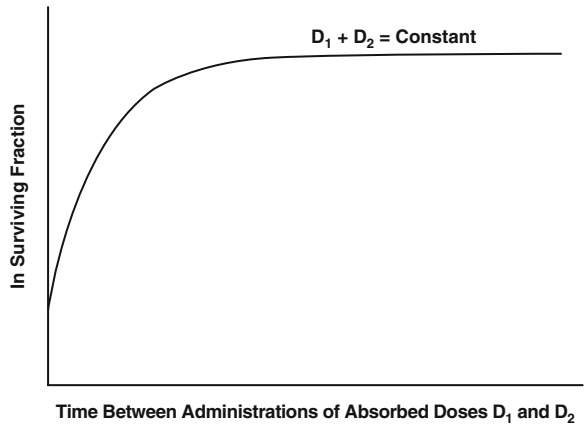

Fig. 10.9 The natural logarithm of the SF of cells irradiated to a constant absorbed dose separated into two separate administrations as a function of the time difference between the administrations of the two absorbed doses

Potentially Lethal Damage

This category of radiation-induced damage is somewhat more complicated than sublethal damage to define. Potentially lethal damage is that which would result in cell death was it not for some postirradiation modification of the cellular environment. In particular, if the cell cycle should be delayed prior to mitosis due to, for example, suboptimal growth conditions, the cell is provided with the opportunity to repair DNA damage. This mode of repair can be important for tumor cells which are quiescent due to a reduced nutritional support from neovasculature leading to an inherent radiation resistance.

10.2.5 Germ-Cell Damage

10.2.5.1 Introduction

Radiation-caused damage to a germ cell can be manifested in two ways. The first is through mutations which can be conferred to the irradiated individual's progeny following fertilization via an inherited genetic defect. These mutation-regulated defects caused by ionizing radiation are no different than those that appear naturally: only the frequency of mutations increases with exposure to ionizing radiation. As a result, it is only possible to detect radiation-induced hereditary effects by comparing the incidences of these effects in the progeny of an irradiated population against those in the progeny of a matched unirradiated population. Because of the low gonadal absorbed doses associated with medical imaging procedures, including diagnostic nuclear medicine, such hereditary effects have not been detected.

The second means of expressing radiation damage to the germ cell is that which leads to germ-cell lethality resulting in either permanent or temporary sterility. Temporary sterility in the male is a theoretically possible sequela of therapeutic nuclear medicine due to the high activity of radionuclide administered and should there be a sufficiently high testicular uptake of the radionuclide.

In this subsection, the latter effect only is considered. Hereditary effects attributable to ionizing radiation are discussed later in this chapter.

10.2.5.2 Oogenesis

In the adult human female, there are approximately 10^5 oocytes. These cells are nonproliferative and, consequently, permanent sterility through radiation-induced ovarian failure can be achieved through the deaths of all oocytes. The magnitude of the absorbed dose required to induce this is highly dependent upon age because, as the female ages, the number of oocytes decreases due to inherent degeneration and, to a lesser degree, ovulation. As a result, the absorbed dose required to cause permanent sterility will be lower in older women than in younger. For example, a typical sterilization absorbed dose to the ovaries in a prepubertal female is about 12 Gy whereas that in a premenopausal female is only about 2 Gy. It should also be noted that hormonal effects typical of the natural menopause accompany radiation-induced sterility.

10.2.5.3 Spermatogenesis

The adult human male gonadal kinetics is markedly different from those of the female, a result of which is the substantially different radiation response between male and female germ cells. Unlike oogenesis, production of sperm cells is a continuous process and spermatazoa are the end-product of several stages in which the spermatogonia (stem cells) lead through sequential differentiation to spermatocytes, spermatids and, finally, spermatozoa. This production process takes about 10 weeks in the human. As with all rapidly dividing cells, spermatogonia are more sensitive to radiation than the further-developed germ cells. This results in the effect of irradiation upon male reproductive capacity not necessarily being immediately evident. Following exposure to irradiation, the male may be only temporarily infertile as the mature sperm cells can remain unaffected. As these are depleted, azoospermia results and temporary sterility exists until the spermatogonia are able to repopulate. Azoospermia can occur for absorbed doses in excess of about 0.5 Gy and its duration is dependent upon the magnitude of the absorbed dose, ranging from about 1 year for absorbed doses of less than 1 Gy to about 3 years for absorbed doses exceeding 2 Gy. Permanent male sterility results for absorbed doses exceeding about 5 Gy given in a single exposure.

10.2.6 In Vitro Cell Survival Curves

10.2.6.1 Introduction

At the level of absorbed doses typical of medical imaging exposures where mitotic death is dominant, cell death is manifested by the lack of reproductive ability. Hence, the deaths of individual cells or colonies of cells due to ionizing radiation can be readily assessed through in vitro assays. The measurement of

the fraction of cells that survive following in vitro exposure to ionizing radiation is fundamental to understanding cellular radiobiology and the environment that can affect the radiosensitivity of the cell.

In vitro measurement of a cell's response to radiation requires the excision of the tumor or tissue of interest, the fragmentation of the sample into individual cells which are then seeded into a culture dish with an appropriate growth medium and then incubated. Established cell lines can be formed in such a way and it is possible to extricate a number of cells using trypsin to cause the cells to detach from the dish. The cell number density (number of cells per unit volume of medium) can then be measured using, for example, a hemocytometer. As a result, a given number of cells can then be seeded in a growth medium, incubated and then viewed, following staining, after a period of about 10 days. Each individual cell has the potential to be clonogenic, i.e., to grow to form a colony which, when stained, is readily visible to the naked eye. The efficiency with which seeded cells eventually form colonies is defined as the plating efficiency,

$$\varepsilon_P = \frac{\text{Number of colonies}}{\text{Number of seeded cells}}. \tag{10.1}$$

ε_P is measured using an unirradiated culture and it is assumed that the plating efficiency is constant across the seeded cultures and is independent of radiation absorbed dose. In a radiobiology experiment, a number of cell cultures are formed and exposed to ionizing radiation. As each colony is the product of a single cell, the SF, accounting for the plating efficiency, represents the fraction of original cells that remain viable following irradiation,

$$\text{SF} = \frac{\text{Number of colonies}}{\text{Number of seeded cells} \times \varepsilon_P}. \tag{10.2}$$

The practical evaluations of (10.1) and (10.2) are shown in Fig. 10.10.

It is important to recognize that the SF is not only a function of the singular absorbed dose, but also of a wide variety of radiation and environmental factors which we shall explore shortly. Hence, the bridging from in vitro experimentation to the prediction of in vivo response must account for such factors which can evolve in the in vivo environment. In the following subsections, a variety of mathematical models of the probability of cell lethality following irradiation are developed.

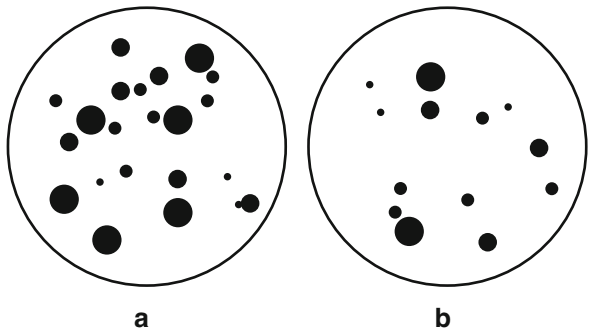

Fig. 10.10 Definitions of plating efficiency and survival fraction determined in vitro. (**a**) Control Petri dish not exposed to radiation; 25 single cells were seeded into it and 22 colonies have been produced resulting in a plating efficiency of $22/25 = 88\%$. (**b**) Petri dish in which 25 cells were also seeded followed by irradiation to yield 13 colonies; the resulting survival fraction is $13/(25 \times 0.88) = 0.591$

10.2.6.2 Single-Target Model

The first model of cell killing by ionizing radiation is the simplest in which a single deactivation (or *hit*) of some target within the cell is sufficient to result in cell death. To derive such a model, recall the Poisson discrete probability distribution function,

$$p(x;\mu) = \frac{\mu^x e^{-\mu}}{x!} \tag{10.3}$$

which gives the probability of x events occurring during a measurement interval for which the mean number of occurrences is μ. The probability of no events occurring (i.e., $x = 0$) during that interval is equal to $e^{-\mu}$. Hence, as the probability of no target deactivation must be equivalent to the probability of survival in this model, one can write the SF of cells following exposure to an absorbed dose D as,

$$\text{SF}(D) = e^{-(D/D_0)} \tag{10.4}$$

where $1/D_0$ is a constant of proportionality. It follows that D_0 is the absorbed dose at which the SF is equal to $e^{-1} \approx 0.37$. An example of a cell survival curve calculated for the single-target model with $D_0 = 0.25$ Gy is shown in Fig. 10.11. On the semilogarithmic plot

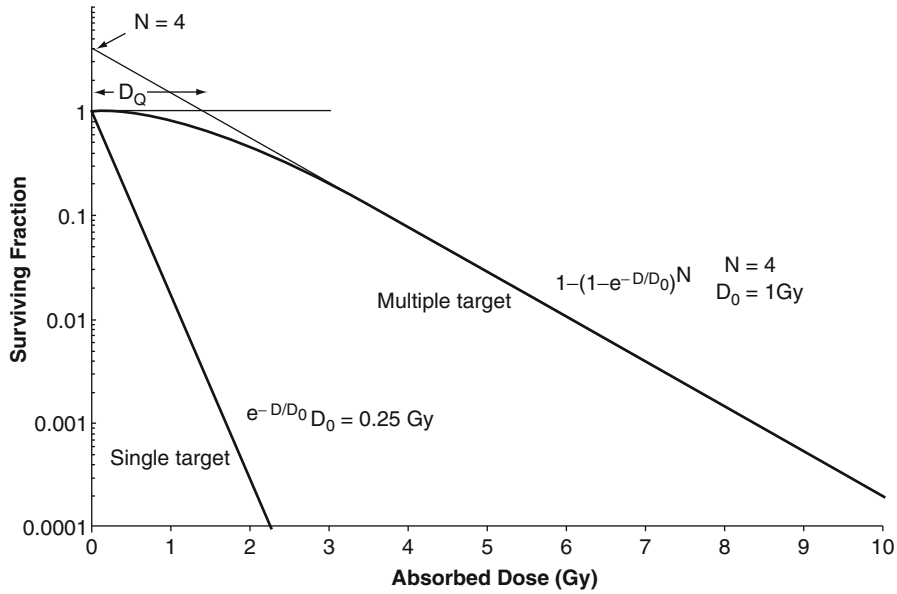

Fig. 10.11 Examples of cell survival curves calculated for the single-target model and a multiple-target model

(10.4), is a straight line reflecting a continuous killing of cells with absorbed dose. As to be shown, such a response reflects the lack of any cellular repair of radiation-induced damage. Such a survival curve is representative of the dose response to high-LET radiations (e.g., α particles) or high absorbed dose rates.

10.2.6.3 Multiple-Target Models

There is no immediate reason to assume that, under all conditions, a radiation-induced hit is sufficient to result in cell death. Table 10.1 would suggest that multiple lesions are required for cell death. Thus, consider the potential of cell death to be due to the inactivation of more than a single target. Equation (10.4) gives the probability that a single target is not hit; hence, the probability that the target is hit is equal to $1 - e^{-D/D_0}$. Assuming that N targets are required to be deactivated in order to cause cell death and that these inactivations are statistically independent, then the probability that cell death results from the N targets being hit is simply $\left(1 - e^{-D/D_0}\right)^N$. The probability of N targets not being deactivated is equal to the SF,

$$SF(D) = 1 - \left(1 - e^{-D/D_0}\right)^N \qquad (10.5)$$

It is clear that (10.5) reduces to the single-hit form of (10.4) for $N = 1$, as required. Figure 10.11 displays a plot of a hypothetical multiple-hit survival curve following (10.5) for an example of four inactivation targets ($N = 4$) and $D_0 = 4$ Gy. The curve has a shoulder at low absorbed doses and an initial slope of zero but which becomes exponential with increasing absorbed dose. At such high absorbed doses, the SF can be written as (using a binomial expansion),

$$SF(D) \approx Ne^{-D/D_0} \qquad (10.6)$$

As a result, the extrapolation of the curve at high absorbed doses back to $D = 0$ will give the number of assumed targets, N, required for cell inactivation. This is shown in Fig. 10.11. A measure of the width of the shoulder is provided by the so-called quasithreshold absorbed dose, D_Q, which is defined as the absorbed dose at which the extrapolation of (10.6) is equal to 1,

$$D_Q = D_0 \ln N \qquad (10.7)$$

This cannot be considered to be a real threshold absorbed dose as radiation damage will still occur at absorbed doses below D_Q. However, D_Q does provide a measure of the survival curve's shoulder at low absorbed doses that is observed in the experimental measurements of many types of mammalian cells.

10.2.6.4 Modified Multiple-Target Model

Measured mammalian cell survival curves indicate that there is in fact a nonzero slope at absorbed doses approaching zero. Contrary to this observation is that the slope of (10.5), expanding the exponentials to first order, is

$$\frac{dSF}{dD} = -\frac{N}{D_0}\left(\frac{D}{D_0}\right)^{N-1}\left(1-\frac{D}{D_0}\right) \qquad (10.8)$$

which is equal to zero for $D = 0$. An improved fit to measured cell survival curves is obtained by incorporating the single-hit model,

$$SF(D) = e^{-D/D_0}\left(1-\left(1-e^{-D/D_1}\right)^N\right). \qquad (10.9)$$

At low absorbed doses, the slope of this modified multiple-target is, again using the first-order expansions of the exponentials,

$$\frac{dSF}{dD} = -\frac{1}{D_0} \qquad (10.10)$$

An example of a cell survival curve of this form is shown in Fig. 10.12 in comparison with the multiple-target model survival curve.

It will be noted that all three dose–response models presented so far asymptotically approach an exponential function of dose with a negative slope in agreement with radiobiological data.

10.2.6.5 Linear-Quadratic Model

Another approach to modeling the cellular response to irradiation is to recall from the discussion of chromosomal aberrations that radiation-induced mutations or cell lethality can result from a DSB produced by a single "hit," where a single ionization event leads to a lesion, or by two independent "hits," where two separate ionization events at different times but occurring in close physical proximity to each other interact to form a DSB. This latter means of lesion induction requires a second-order dose-dependent component to the probability of cell survival, or,

$$SF(D) = e^{-(\alpha D+\beta D^2)} \qquad (10.11)$$

where α and β are constants. This is the linear-quadratic (LQ) model (Fowler and Stern 1960). An example of a hypothetical LQ cell survival model is shown in Fig. 10.13, along with the multiple-target example survival curve.

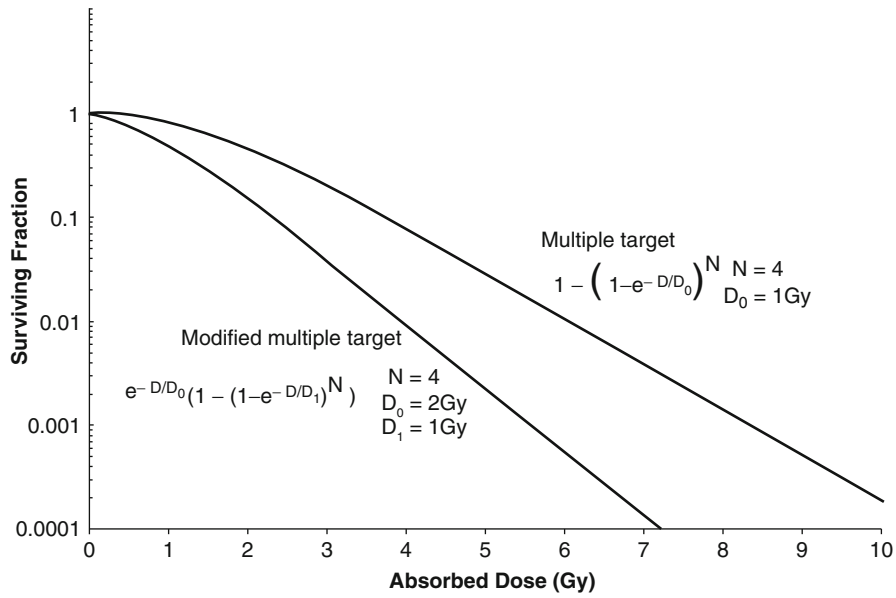

Fig. 10.12 Examples of multiple target and modified multiple-target survival curves. Note that the modified multiple-hit survival curve has a nonzero slope at $D = 0$

A significant problem that occurs with (10.11) at high absorbed doses is that the LQ model never approaches the pure e^{-D} dependence which is observed experimentally. This failure will tend to restrict the utility of the model to low absorbed doses where it does present an advantage over other models in that it requires only two parameters to enable a fit to measured radiobiological data. The ratio of the α and β parameters is equal to the absorbed dose at which the contributions of the linear and quadratic components are equal,

$$D_{Eq} = \frac{\alpha}{\beta}. \tag{10.12}$$

The coefficients of the LQ model can be determined from measured cell survival curves through (10.11),

$$-\frac{\ln SF}{D} = \alpha + \beta D. \tag{10.13}$$

A plot of D vs. $\ln SF/D$ will thus yield the coefficients of the LQ model where α is the intercept and β is the slope.

As the quadratic component represents cell lethality due to two DSB-inducing ionizations separated in time, one must allow for the possibility of the repair of the first sublethal DSB during the time before the second DSB occurs. This process will increase the SF over time. Should this second DSB occur before the repair of the first, the result is cell death. The inclusion of this sublethal damage repair is enabled by writing the LQ model of the survival fraction of (10.11) as,

$$SF(D) = e^{-\left(\alpha D + \beta G D^2\right)}. \tag{10.14}$$

G is the Lea–Catcheside factor where $G \leq 1$ and accounts for the reduction in cell lethality due to the repair of sublethal damage. This factor will obviously be a function of the difference in times between when the first radiation insult occurs and that of the second.

The LQ model has been extensively used in applications of clinical radiobiology to external beam radiotherapy, brachytherapy, and radionuclide therapy.

10.2.7 Radiation Sensitivity of Mammalian Cells

10.2.7.1 Introduction

The response of a given cell to radiation is a function of many biological, physical, and environmental variables such as cell cycle, the rate at which the radiation

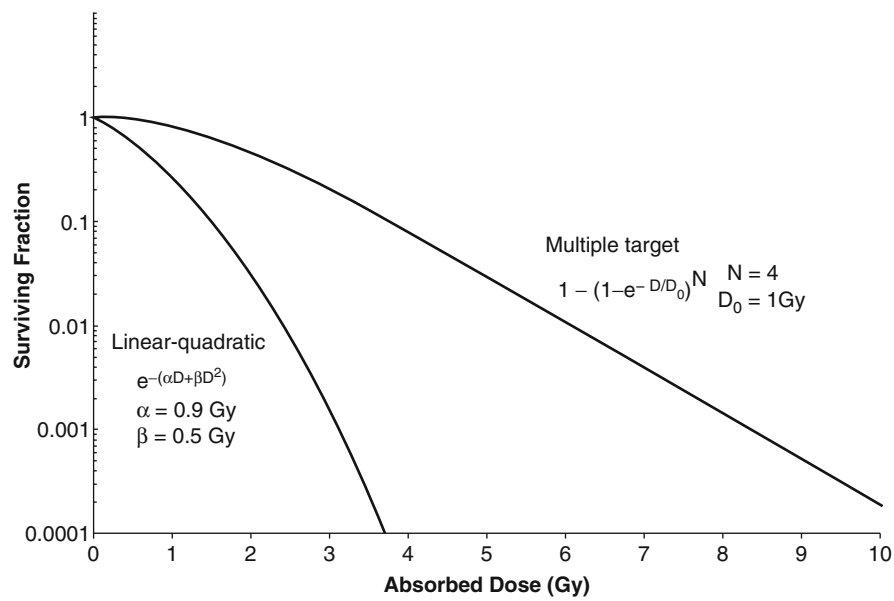

Fig. 10.13 Hypothetical cell survival curves for the multiple-target and linear-quadratic models. Note that the slope of the linear-quadratic curve in this semilogarithmic plot never approaches a straight line (i.e., it is not pure exponential), in contradiction to measured cell survival curves

absorbed dose is delivered and the ambient oxygen concentration. The last two factors are of particular importance in radionuclide therapy.

10.2.7.2 Cell Cycle and Age

The cell cycle, as defined by the period of time between subsequent mitoses, was introduced in Sect. 10.2.2.5. The sensitivity of the cell to radiation varies throughout the course of the cycle. The length of the G_1 phase, which precedes the DNA synthesis S phase, is indicative of the variation of the radiosensitivity of the cell throughout its cycle. Figure 10.14 shows two conceptual mammalian cell proliferative capacities and how they vary with the time of the cell cycle at which they receive the same absorbed dose. The cells are the most radiosensitive during the mitosis phase. For cells with long G_1 phases, the cell is relatively radioresistant during much of the course of G_1 but this sensitivity decreases as the G_1 phase enters the synthesis S phase; the radioresistance again increases to a maximum during the S phase and then decreases through the G_2 and M phases. On the other hand, for cells with short G_1 durations, radioresistance increases through the M and G_1 phases to reach a single maximum during the S phase to again decrease during the G_2 and M phases.

This variability of radiosensitivity throughout the cell cycle enables the process of synchronization. Proliferative cells in situ or in culture will exist in different stages of the cell cycle without any synchronicity between them. Following irradiation, those cells which are in the radiosensitive phases will be preferentially killed whereas those in the radioresistant S phase will survive. Hence the culture of cells will, following irradiation, tend to be at the same phase of the cell cycle.

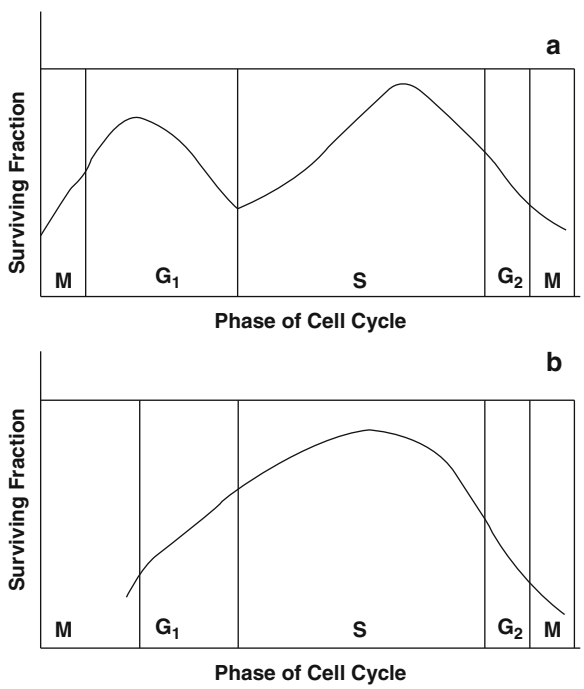

Fig. 10.14 Conceptual plots of mammalian cell survival, for two categories of (**a**) long and (**b**) short G_1 phases, for the same absorbed dose as a function of the phase of the cell cycle during which it was irradiated

10.2.7.3 Relative Biological Effectiveness

The relative biological effectiveness (RBE) is a measure of the difference between the incidence or magnitude of biological effects incurred by exposure to a given radiation type or set of irradiation conditions relative to a low-LET reference radiation (commonly, the secondary electrons associated with 250 kVp X-rays) for a given biological endpoint, which is typically the survival fraction. This definition is shown in Fig. 10.15. An important point to note is that the RBE is a function of the endpoint selected, as can be seen by comparing the RBE values defined by 0.1 and 10% cell survivals.

10.2.7.4 Linear Energy Transfer

As described in Chap. 7, the linear energy transfer (LET) is a measure at which energy is deposited in a medium per unit length of travel by a charged particle. Increasing values of LET correspond to increasing ionization densities. The result is that, increasing LET (e.g., increasing from those of Compton electrons and photoelectrons through Auger/Coster–Kronig electrons to α particles), the probability of killing the irradiated cell will grow. That is, in terms of the cell survival curve, increasing LET will result in a reduction in the curve's shoulder and an increase in its slope, as shown in Fig. 10.16. These are the results

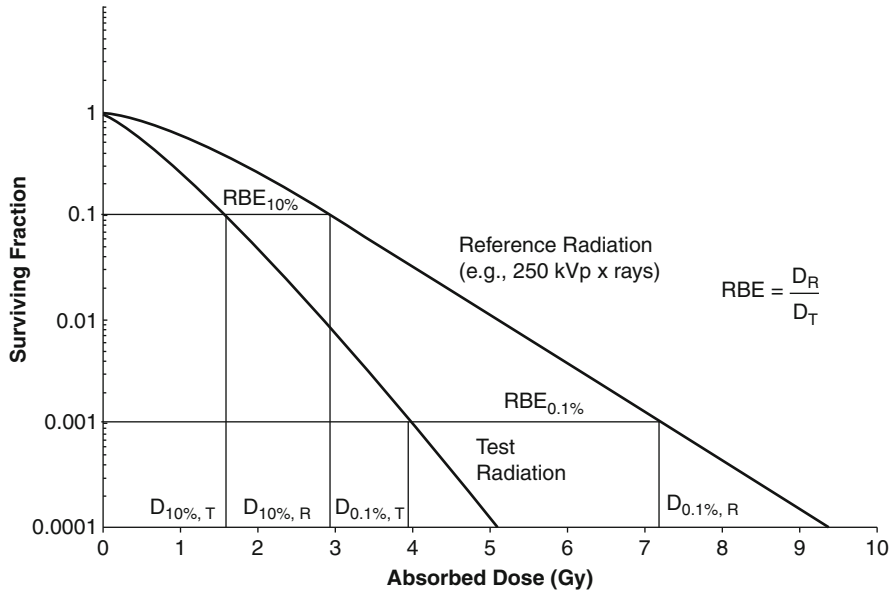

Fig. 10.15 Definition of the relative biological efficiency (RBE) as the relative reduction in absorbed dose from a specified low-LET reference radiation type for a test radiation/irradiation conditions to yield a given endpoint (here, cell SF). Note that the value of the RBE is dependent upon the endpoint selected (here, $RBE_{0.1\%} > RBE_{10\%}$)

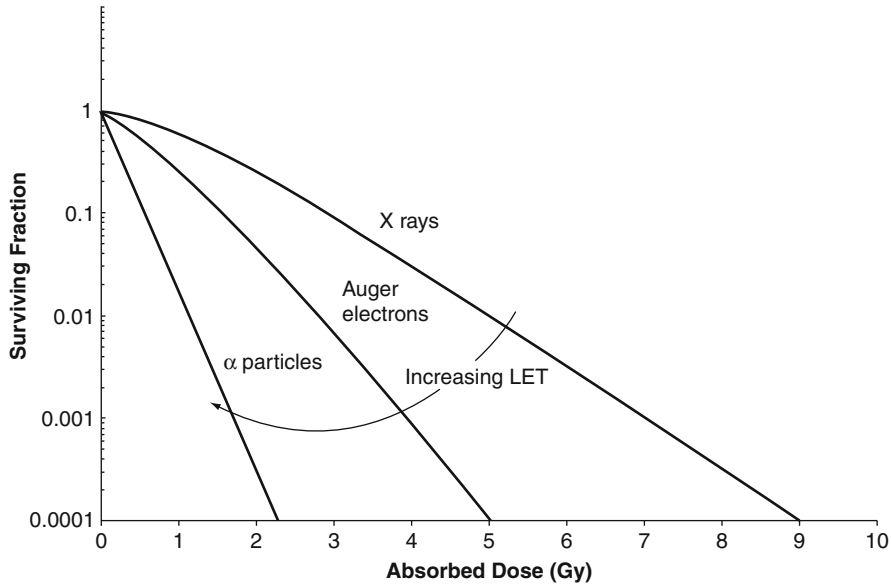

Fig. 10.16 Conceptual set of cell survival curves for radiations of varying LET values. Note that with increasing LET, the slope of the curve increases (becomes more negative) and the shoulder decreases

of a high incidence of cell killing and a reduced opportunity provided for sublethal damage repair.

10.2.7.5 Absorbed Dose Rate

Of importance to radionuclide therapy is the variation in biological response with absorbed dose rate. For a given fixed absorbed dose, the functional survival will decrease with an increase in the rate at which the dose is delivered. This is shown conceptually in Fig. 10.17. As a result of sublethal damage repair, the cell has a greater opportunity to restitute a DSB at low absorbed dose rates and the cell survival curve subsequently demonstrates a shoulder at low absorbed doses and a reduced slope. As the absorbed dose rate increases thus increasing the rate at which DSBs are produced, the ability of the cell to "keep up"

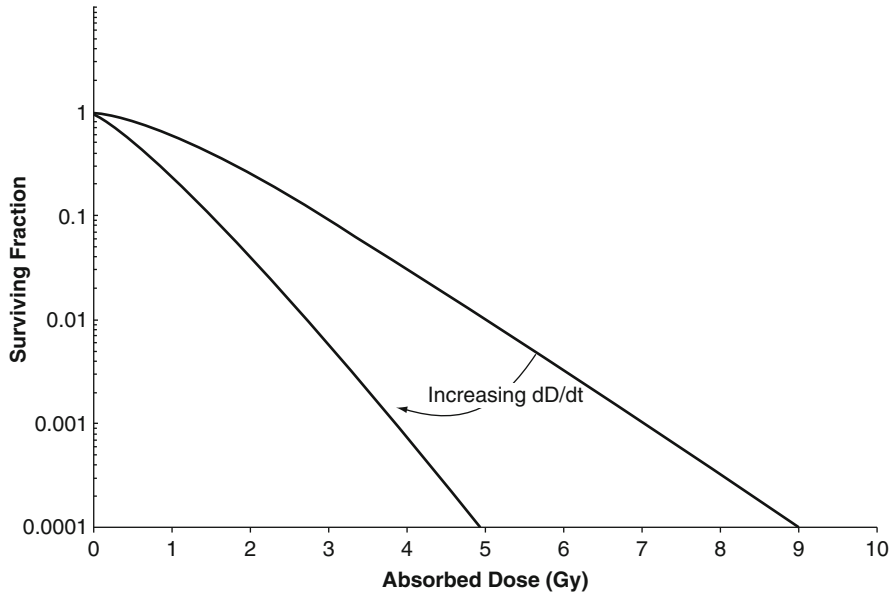

Fig. 10.17 Conceptual cell survival curves for identical low-LET radiation type but at different absorbed dose rates, dD/dt. For a fixed total administered absorbed dose, the fractional survival decreases with increasing absorbed dose rate due to the impairment of cellular repair of DNA damage

and repair DSBs as they are produced is diminished. The SF decreases as a result and the shoulder of the cell survival curve shortens and the slope increases.

Similar to the concept of varying the rate of a continuous exposure of ionizing radiation s the application of radiation administered in separated integral exposures, known as fractions. This permits irradiated normal tissue to repair between fractions. Figure 10.18 shows hypothetical dose–response curves for fractionated therapy with a time interval between each fraction sufficient to allow the repair of sublethal damage. The dashed line is the net dose response resulting from single exposures of 1 Gy each.

10.2.7.6 Hypoxia

In the discussion of indirect radiation-induced damage of the DNA, it was noted that the presence of oxygen can increase the radiosensitivity of the mammalian cell by impeding the immediate recombination of ion pairs following an ionization, thus "fixing" the presence of the free radicals produced by the ionization. Hypoxic conditions thus decrease the radiosensitivity of the cell, a feature which is of great practical concern in radiotherapy as a tumor frequently contains hypoxic regions.

A measure of this effect of oxygen concentration upon radiosensitivity is the *oxygen-enhancement ratio* (OER) defined as the ratio of the absorbed dose required to achieve a specified biological endpoint (e.g., survival fraction) under hypoxic conditions to that achieving the same endpoint under aerated conditions, as shown in Fig. 10.19.

10.2.7.7 RBE and OER as Functions of LET

Having now seen how fractional cell survival varies with OER and LET, it is of interest to see how both the RBE and OER vary with LET. Figure 10.20 shows hypothetical RBE and OER curves as functions of LET (although hypothetical, they demonstrate qualitatively those functions shown in Barendsen et al. (1966) and Barendsen (1968)).

The OER has a value of about 2.5–3 for low-LET radiations, but drops off precipitously for LET values in excess of about 30 KeV/μm to eventually "plateau" to reach unity at about 200 KeV/μm. On the other hand, the RBE has limited energy dependence, staying equal to unity with LET values less than about 10 KeV/μm, to reach a sharp maximum at about 100 KeV/μm before decreasing. At low values of LET, the number of ionizations is decreased and the presence of oxygen can fix the produced free

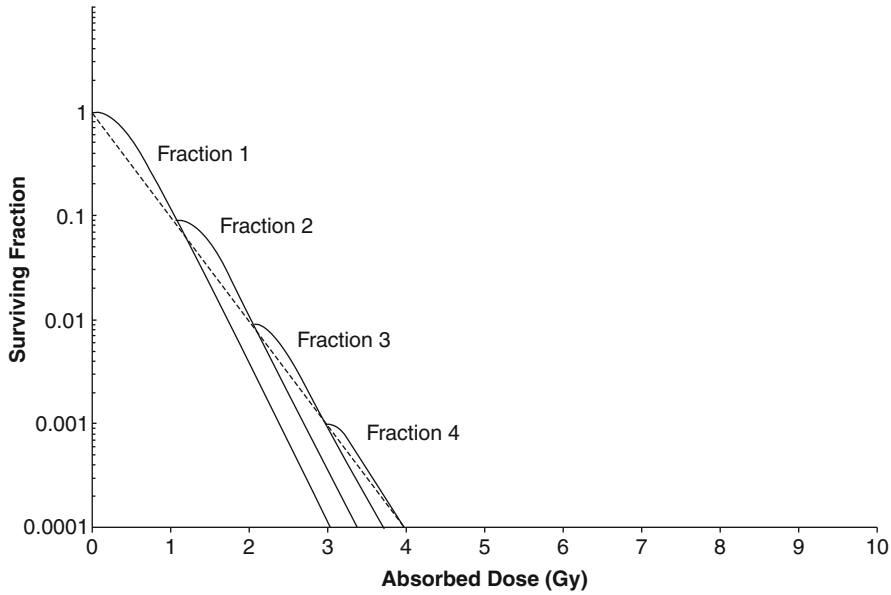

Fig. 10.18 Hypothetical dose–response curves for fractionated exposure. The cell survival is 10% for a single exposure of 1 Gy. The exposure is split into four fractions, each providing 1 Gy. The *solid lines* indicate the SFs resulting from an absorbed dose administered at a single time. The *dashed line* is the dose response obtained if the absorbed dose is administered in fractions of 1 Gy each. It can be seen that the SF for a given total absorbed dose is greater if the absorbed dose is given as smaller, fractionated exposures (e.g., 0.01% of the cells survive a 3 Gy absorbed dose given in a single exposure whereas 0.1% survive the same absorbed dose if given in three fractions)

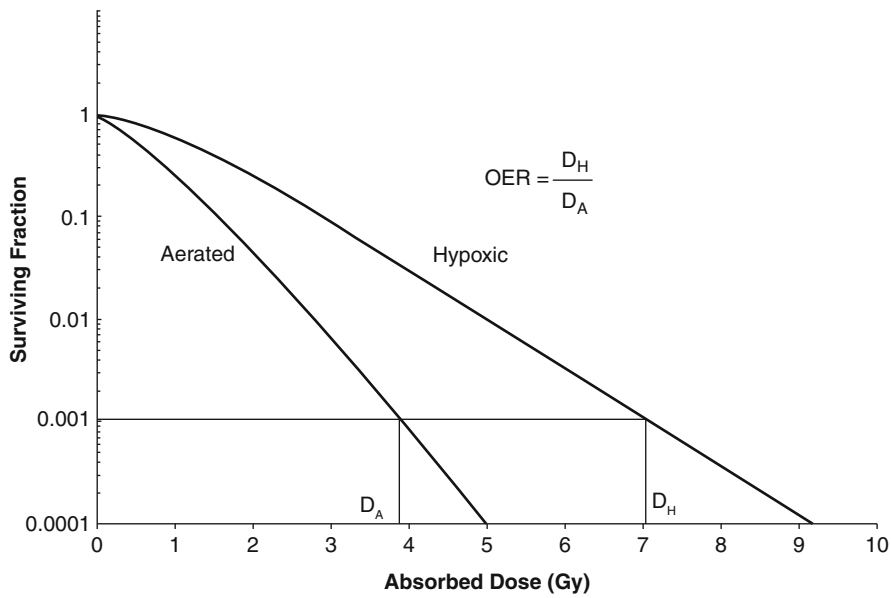

Fig. 10.19 Effect of hypoxia upon cell SF and the definition of the oxygen-enhancement ratio (OER) for two hypothetical cell survival curves; the endpoint used is arbitrary

radicals and, hence, the consequential OER is high. At high LET values, the ionization density within the intranuclear medium is sufficiently high that oxygen repair of indirect damage is insufficient and indirect damage is inhibited. The RBE remains relatively constant at low-LET values due to the large mean physical separation between ionization events. Because of this, the probability that an ionization will damage DNA through either direct or indirect mechanisms is small. At high LET, the separation between ionization events is small and the density of ionizations correspondingly higher so as to elevate the probability of an ionization near the DNA molecule leading to the increase in the damage incurrence

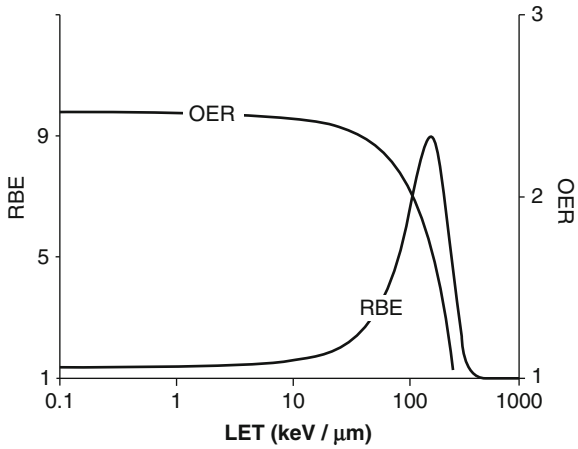

Fig. 10.20 Conceptual curves of OER and RBE as functions of LET. Note different ordinates for the quantities of interest

rate. The peaking of the RBE at about 100 KeV/μm can be explained by noting that the mean separation between energy deposition events at an LET value of 100 KeV/μm is about 2 nm, which, of course, is of the order of the DNA double helix's diameter. Hence, at this LET value, there is a high probability of a single charged particle inducing a DSB in the helix which can lead to cell death. At lower LET values, the mean separation between events is greater and the probability of a DSB occurring is correspondingly reduced. The decrease in RBE with LET increasing beyond 100 KeV/μm reflects "overkill" by densely-ionizing radiation. Multiples of DSBs are produced, but the increase in biological effect is limited whereas the absorbed dose increases with the net result that the RBE decreases. This RBE maximum at an LET value of 100 KeV/μm is of particular interest to therapeutic nuclear medicine of α-emitting radionuclides. From Table 10.2, it can be seen that the typical LET of the α particles emitted from a radionuclide is between 100 and 150 keV/μm and which is coincident with this RBE maximization and the minimization of the OER.

10.2.7.8 Cell Proliferation Kinetics and Radiosensitivity

The variation of cell sensitivity to ionizing radiation due to its proliferative capacity is of significant interest to both the induction of cellular effects and the minimization of radiation-induced sequelae. Tumor cells rapidly proliferate as do the blast cells of some normal tissues and, hence, would be expected to have comparable radiosensitivities.

It is possible to categorize normal cells in terms of their proliferation capacities:

No mitosis	Neurones
Low mitotic rate/limited cell renewal	Thyroid, liver, and connective tissue
High mitotic rate/ frequent cell renewal	Red bone marrow (erythroblasts), spermatogonia, and intestinal crypt cells

The sensitivity of a given cell to damage induced by ionizing radiation is commensurate with its proliferative capacity. Cells with a high mitotic index, which includes tumors, are particularly sensitive to ionizing radiation; those cells with a low mitotic index tend to be less radiosensitive.

Table 10.2 Typical values of LET and particle ranges

Particle	Typical LET (keV/μm)	Typical range (μm)
Secondary electrons resulting from Compton and photoelectric interactions with photons of energies typical of nuclear medicine	2–5	5,000
Electrons and positrons emitted in β decay	1	50–2,500
Auger/Coster–Kronig electrons	50	0.01
α particles emitted in α decay	100–150	50–100

10.2.8 Repair of Radiation-Induced Damage

10.2.8.1 Introduction

It has been estimated that the DNA of a single mammalian cell will experience normally some 10^5 lesions daily as the consequence of a variety of insults including replication errors, attacks by reactive chemical species or ionizing radiation. The fact that the natural mutation rate is so low demonstrates that intrinsic

DNA repair mechanisms exist. These mechanisms are applied at different phases of the cell cycle.

10.2.8.2 Repair of Sublethal Damage

Sublethal damage repair reflects the increase in cell survival if a given amount of absorbed dose is administered in multiple exposures rather than in a single one. Figure 10.21 shows a conceptual description of mammalian cell survival following two exposures (yielding the same total absorbed dose) separated by a time interval. The SF initially grows with increasing time between the two irradiations, reflecting the repair of sublethal damage caused by the first exposure (referred to as the conditioning dose). However, after about 2–4 h, the SF decreases to a minimum and then begins to increase again. This phenomenon is the result of radiation-induced synchronization, described in Sect. 10.2.7.2. As mammalian cells are most radioresistant during the S phase of the cell cycles so of a culture of cells irradiated in situ, the surviving cells will tend to be in the S phase.

After 6 h, the cells will be in the G_2/M phases which are radiosensitive. Irradiation during this time will decrease the SF; this is known as reassortment. At later times, the number of cells increases due to further cell divisions (repopulation).

10.2.8.3 The Four "Rs" of Radiobiology

The above discussions can be summarized by what are known as the four "Rs" of radiobiology and their applicability to fractionated or low-dose irradiation using low-LET radiation in radiotherapy.

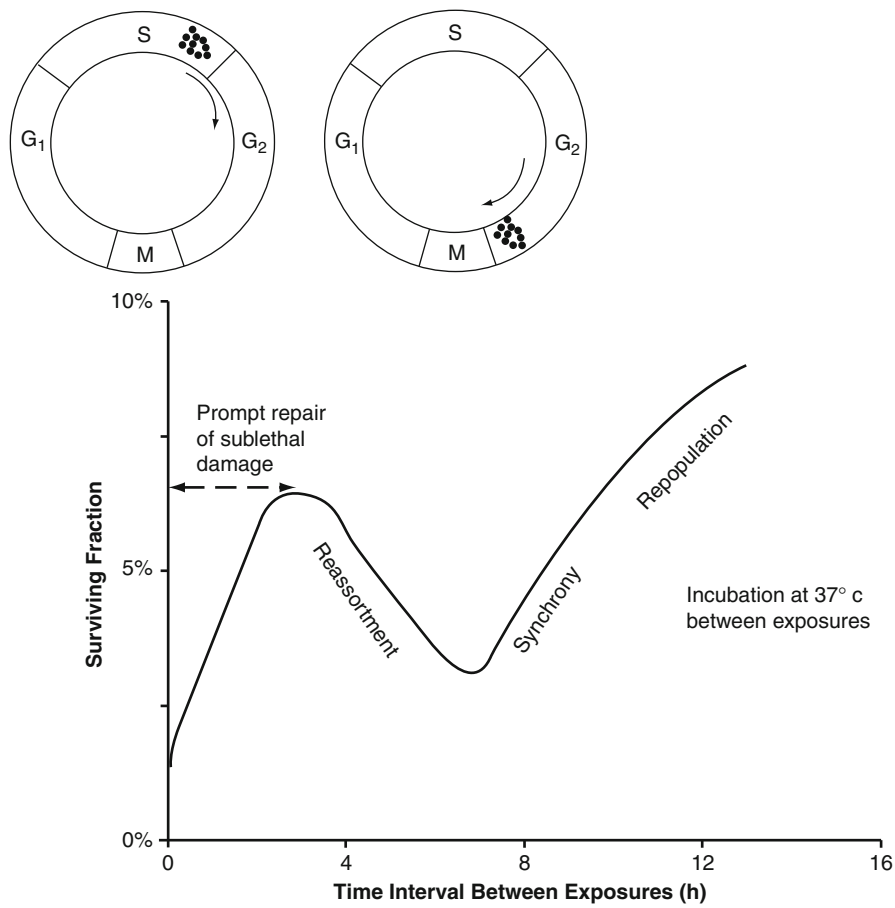

Fig. 10.21 SF of mammalian cells exposed to two fractions of radiation and incubated at 37°C for various lengths of time between the two exposures. Figure follows from Hall and Giaccia (2006). Refer to text for description

Repair of sublethal damage – The repair of sublethal damage occurs during the first few hours of lesion induction.

Reassortment – As shown in Fig. 10.20, subsequent irradiations of a cell population will preferentially lead to the dominance of radioresistant cells in the irradiated population.

Repopulation – This is a special concern in fractionated therapy. Tumor cells can repopulate between administration fractions, which is not desirable. On the other hand, repopulation of normal cells during these intervals is desirable so as to limit the normal tissue complication rate.

Reoxygenation – Reoxygenation is conceptually demonstrated in Fig. 10.22 in terms of the irradiation of a tumor cell.

In short, low-dose or fractional irradiation will spare normal tissue through the allowance of repair and repopulation; it will also allow the increased damage to tumor cells through reoxygenation and the reassortment of tumor cells into their radiosensitive phases. These results need to be reflected in the various considerations of radionuclide therapy. The extension of treatment time results in the reduction of immediate reactions of normal tissues to irradiation and, as demonstrated in Fig. 10.22, the reoxygenation of tumors and to increase their radiosensitivity.

10.2.9 Radiation-Induced Mutations

10.2.9.1 Introduction

The low absorbed doses associated with diagnostic nuclear medicine studies set the risks to the irradiated individual to be the probabilistic risks of radiocarcinogenesis and hereditary effects due to the induction of mutations. Tissue homeostasis is the outcome of the combination of controlled cell division and apoptosis. A tumor lacks these attributes and the progression from normal tissue to tumor is the result of mutations to three categories of genes (Hall and Giaccia 2006):

- The proto-oncogene which, in normal fashion, is a positive growth factor but, following mutation, produces an oncogene that ignores extracellular signals that would inhibit division.
- Tumor-suppressor genes (e.g., p53) which are negative growth factors.
- DNA stability genes which allow sensing of DNA damage and repair.

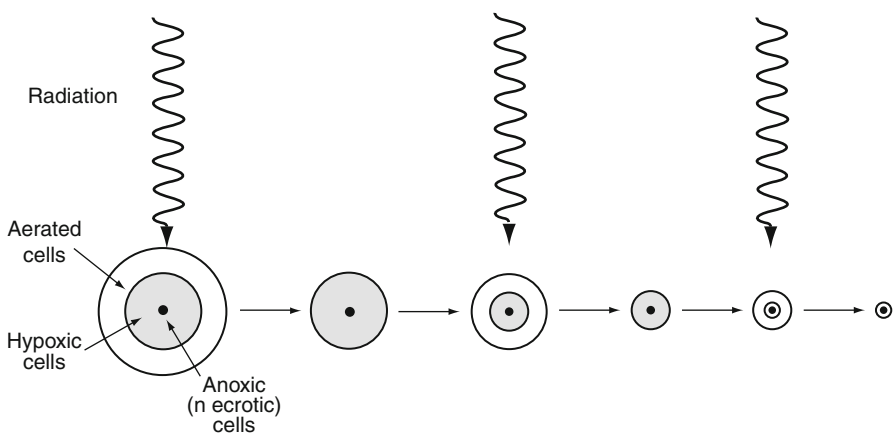

Fig. 10.22 The concept of reoxygenation in the fractionated/low absorbed dose rate therapy of a tumor. Due to inadequate vascularization, the tumor will have a necrotic core surrounded by a shell of hypoxic cells which is further surrounded by aerated cells in response to the degree of the radial dependence of vascularization and oxygen tension. Due to the oxygen-enhancement effect, radiation will preferentially kill the circumferential aerated cells leaving the hypoxic cells at the end of treatment. Following exposure, vascularization, and oxygenation of the outer rim of the tumor increases to produce aerated cells which are radiosensitive. Again, following irradiation, this outer shell is killed leaving a reduced hypoxic core. The process continues sequentially

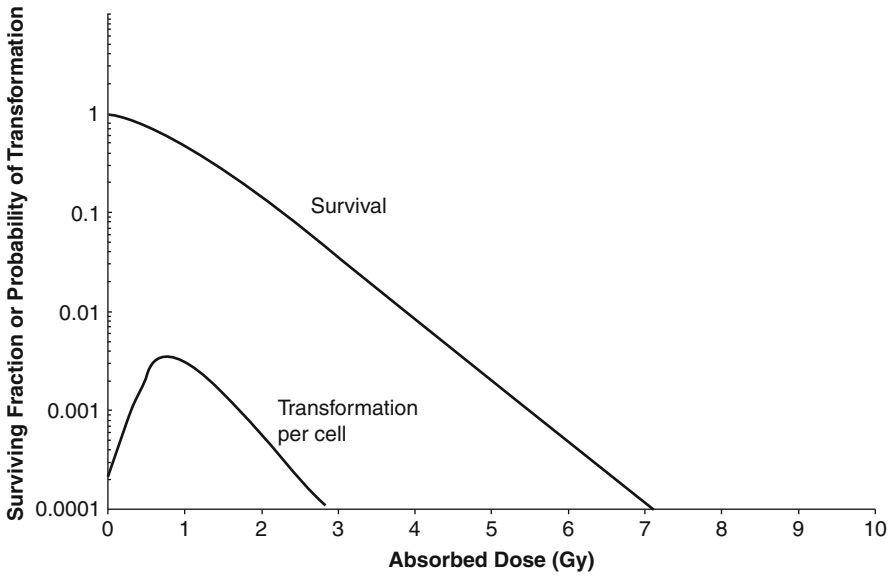

Fig. 10.23 A conceptual plot of the probability of a mutation per cell and the fractional survival of such cells in a population as a function of absorbed dose for low-LET radiation

Figure 10.23 compares the probabilities of survival and mutation as functions of absorbed dose for low-LET radiation. The likelihood of survival decreases exponentially whereas the rate of mutations, however, increases with absorbed dose to a maximum absorbed dose and then decreases with the same slope as that of the cell survival curve. This reflects the death of the mutated cells with increasing absorbed dose.

10.2.9.2 Oncogene Activation

The concept of the oncogene – a gene which can induce cancer – is based upon studies in the early twentieth century which demonstrated that tumors in mice, chickens, and rats were transmissible by the injection of the cell-free filtrate of the tumor into another animal. The transmitting factor has since been determined to be a retrovirus (a virus whose genome is composed of RNA). There are two models of the activation of oncogenes. The first is the viral oncogene model in which the retrovirus enters the cell and its RNA is then integrated into the host cell's genome and the genetic information leads to the synthesis of a protein which leads to a malignant transformation. The second model is that of the activation of proto-oncogenes through mutation. These are, in the first instance, normal genes but which, through mutation, lead to malignancy.

10.2.9.3 Inactivation of Tumor-Suppressor Genes

Uncontrolled growth of cells is inhibited through genes such as p53. A radiation-induced mutation of such a gene can lead to its inactivation followed by uncontrolled cell division leading to a tumor.

10.2.9.4 Germ-Cell Mutations

Mutation-induced activation of an oncogene or inactivation of a tumor-suppressor gene can only affect the individual in which these processes have occurred. The effect of a mutation of a germ cell, on the other hand, is not apparent in the exposed individual but is transmitted to its progeny and, as the mutation now enters the broader gene pool, can affect a multitude of individuals. Hence, radiation-induced hereditary effects have been of great interest as the affected population is much greater than the single exposed person.

Large absorbed doses to germ cells lead to permanent sterility. But at low absorbed doses received by germ cells, the viability of the cell is unaffected, but mutations can be induced. It is important to understand that mutations induced by ionizing radiation and which are expressed as hereditary effects are no different than those which occur naturally; ionizing radiation can only increase the frequency of such mutations and not influence their characteristics.

10.3 The Linear-Quadratic Dose–Response Model for Low-LET Radiation

10.3.1 Introduction

The LQ model was introduced in the discussion of cell survival curves within the qualitative context of a DSB produced by single and double ionizations. In the latter case, the temporal separation between the two separate ionizations allows the lesion to be repaired. Repair may be as simple as recombining the ends of the broken strands. This restitution restores the physical integrity of the helix, but not the original base pair sequence. Binary misrepair can also occur between damaged chromosome pairs. This illegitimate repair can result in the production of a dicentric chromosome and acentric chromosome fragments and centric rings, the latter being predominant.

In this section, the various applications of the LQ model in assessing and predicting tissue responses to radiation are investigated. The four main premises of the LQ formalism are (Brenner et al. 1998):

- The yield of radiation-induced DSBs is proportional to absorbed dose.
- The DSB repair rate is first-order.
- The binary misrepair of DSB pairs produced from two different radiation tracks competes with this first-order repair with a yield proportional to the square of the absorbed dose[3].
- Single radiation tracks can induce lethal lesions with a yield proportional to absorbed dose.

Discussion of the LQ model is limited to low-LET radiations (photons and electrons) where the scarcity of ionizations enables cells to repair radiation-induced damage. High-LET radiations (such as α particles or Auger electrons) have high ionization densities which fail to provide an opportunity for the cell to repair radiation-induced damage (e.g., Fig. 10.15).

10.3.2 DSB Repair Kinetics

10.3.2.1 First-Order Repair Kinetics

The basic kinetics of the induction of radiation-linked DSBs are first presented. Let U(t) be the mean number of DSBs present per cell at a time t following irradiation. If it is assumed that the number of repaired DSBs during a time interval δt is proportional to the total number of DSBs, given by the product $\mu U(t)\delta t$, then solving the first-order differential equation yields,

$$U(t) = U_0 e^{-\mu t} \tag{10.15}$$

where U_0 is the number of DSBs at the end of irradiation and μ is the first-order DSB repair rate constant.[4] Values of μ for most organs are of the order 0.2–1.4/h, corresponding to repair half-lives of between 0.5 and 3 h.

10.3.2.2 Binary DSB Misrepair

Whereas the majority of DSBs can be resolved through restitution in which the two ends of the DSB rejoin, some DSB repairs result in illegitimate binary unions. The rate at which binary misrepair occurs can be deduced by assuming that the probability distribution of the number of DSBs is Poisson. Let θ be the number of DSBs in a cell, where $U = \bar{\theta}$. The number of DSB pairs in the cell will thus be equal to $\theta(\theta - 1)/2$ (where, from the definition of U(t), a dicentric chromosome and the acentric fragments are counted as a single lesion). Each binary misrepair removes two DSBs. If κ is the rate of binary misrepair per DSB pair, the mean DSB-removal rate through binary misrepair is,

$$\begin{aligned} 2\kappa\left(\overline{\theta(\theta-1)/2}\right) &= \kappa\bar{\theta}^2 \\ &= \kappa U^2 \end{aligned} \tag{10.16}$$

[3]The time difference between induction of the two lesions allows the first to be repaired before it would otherwise misrepair with the second.

[4]In some cases, a biexponential temporal behavior in the reduction of DSB number has been observed (Frankenberg-Schwager 1989). This is not considered here.

10.3.2.3 Kinetics of DSB Induction, Repair and Misrepair, and Cell Survival

In this subsection, the kinetics of DSB creation, repair, and misrepair are used to estimate the fraction of surviving cells in a population that has been irradiated. This leads naturally to the LQ expression for this fraction. However, to simplify the derivation, cell repopulation is considered to be negligible. From the premise that the induction of DSB is proportional to dose, the rate equation for the mean number of DSBs in a cell is,

$$\frac{dU}{dt} = \delta\frac{dD}{dt} - \mu U - \kappa U^2 \tag{10.17}$$

where the first term is the DSB creation rate, the second term is the first-order repair rate, and the third term is the binary misrepair rate. δ is the mean number of produced DSBs per unit absorbed dose, the production rate of which is roughly 40 DSB/Gy (Sachs et al. 1997) and dD/dt is the absorbed dose rate.[5] The rate equation for the mean number of cells, N, in an irradiated population is,

$$\frac{dN}{dt} = -\left(\alpha\frac{dD}{dt} + \kappa U^2\right) N. \tag{10.18}$$

The first term of (10.18) describes cell death due to a single ionizing radiation track and the second term describes the rate of cell death as a result of binary DSB misrepair. The κU^2 term is smaller than the other terms of (10.17) for absorbed doses of less than 5 Gy and, for the ease of solving this pair of coupled differential equations, is neglected. However, the corresponding term in (10.18) is not ignored. Neglecting κU^2 and integrating (10.17), the mean number of DSBs per cell is

$$U(t) = \delta\, e^{-\mu t}\int_{-\infty}^{t} dt'\frac{dD(t')}{dt'}e^{\mu t'}. \tag{10.19}$$

Substituting this into (10.18) and integrating, one obtains, at time T, the logarithm of the SF,

$$\begin{aligned}\ln\left(\frac{N(T)}{N_0}\right) &= -\alpha D - \frac{\delta^2\kappa}{2\mu} \\ &\quad\times\left(\frac{2}{D^2}\int_{-\infty}^{T} dt\frac{dD(t)}{dt}\int_{-\infty}^{t} dt'\frac{dD(t')}{dt'}e^{-\mu(t-t')}\right)D^2 \\ &= -\alpha D - \beta G D^2\end{aligned} \tag{10.20}$$

where $\beta \equiv \delta^2\kappa/2\mu$ and G is the Lea–Catcheside dose-protraction factor (Lea and Catcheside 1942) which describes the damage repair occurring between two separate ionizations. This factor is less than or equal to unity and is developed further in the following subsection. Equation (10.20) is the LQ model, modified so as to account for repair of sublethal damage.

Further examination of the β factor is of interest. It is proportional to the square of the mean number of DSBs induced per unit absorbed dose (δ), reflecting the effect of two independent ionizations. It is also proportional to the rate of binary DSB misrepair per DSB pair and inversely proportional to the first-order repair rate.

10.3.2.4 Lea–Catcheside Dose-Protraction Factor

The Lea–Catcheside factor is written in the more general form,

$$G = \frac{2}{D^2}\int_{-\infty}^{\infty} dt\frac{dD(t)}{dt}\int_{-\infty}^{t} dt'\frac{dD(t')}{dt'}e^{-\mu(t-t')} \tag{10.21}$$

where

$$D = \int_{-\infty}^{\infty} dt\frac{dD(t)}{dt} \tag{10.22}$$

The integrand of the second integral over t' refers to the first of the two DSBs required to cause lethality; the exponential term describes the repair and subsequent

[5] "Saturable" repair mechanisms have been proposed as another means of describing the curvature of the LQ dose-response curve (e.g., Goodhead 1985). In saturable repair, μ has an absorbed-dose dependence, decreasing as dose increases and thus leading to a reduced repair efficiency with increased absorbed dose. Brenner et al. (1998) presented a modification of (10.17), $\frac{dU}{dt} = \delta\frac{dD}{dt} - U\sum_{i=1}^{2}\frac{\lambda_i}{1+\varepsilon_i U}$ where the first term in the summation corresponds to the creation of initial lesions and the second term corresponds to the production of lethal lesions from the initial lesions. These terms refer to the saturation of repair (essentially, this is the Michaelis–Menten equation applied to enzyme kinetics).

reduction of such a DSB. The integral over t refers to the second of the two DSBs that interacts with a remaining unrepaired first DSB to cause the inevitable lethal damage. For acute irradiation which does not enable the cell to repair radiation-induced damage, the Lea–Catcheside factor is $G = 1$. However, as the kernel $e^{-\mu(t-t')} \leq 1$ for prolonged irradiation, then $G < 1$ in such cases due to the ability for repair to occur.

The Lea–Catcheside factors for two types of absorbed dose rates are now derived for two cases of relevance.

Constant Absorbed Dose Rate for Finite Irradiation Time

In this case, the absorbed dose rate is given by,

$$\begin{aligned} \frac{dD(t)}{dt} &= R \quad 0 \leq t \leq T \\ &= 0 \quad \text{elsewhere} \end{aligned} \tag{10.23}$$

where R is a constant dose rate, T is the duration time of irradiation and the total absorbed dose is clearly the product of this dose rate and the irradiation time $D = RT$. Then, the Lea–Catcheside factor for this absorbed dose rate is, from its definition,

$$\begin{aligned} G &= \frac{2}{D^2} \int_{-\infty}^{\infty} dt \frac{dD(t)}{dt} \int_{-\infty}^{t} dt' \frac{dD(t')}{dt'} e^{-\mu(t-t')} \\ &= \frac{2}{(RT)^2} \int_0^T dtR \int_0^t dt' \, R \, e^{-\mu(t-t')} \\ &= \frac{2}{T^2} \int_0^T dt \, e^{-\mu t} \int_0^T dt' \, e^{\mu t'} \end{aligned} \tag{10.24}$$

Solving the integrals gives the dose-protraction factor for a constant absorbed dose rate delivered for a finite time T,

$$G = \frac{2}{(\mu T)^2} \left(\mu T + e^{-\mu T} - 1 \right) \tag{10.25}$$

It is straightforward to demonstrate that, by expanding the exponential to second-order, the Lea–Catcheside factor $G \to 1$ as the irradiation time $T \to 0$. In other words, the $\beta G D^2$ contribution to cell lethality increases to βD^2 as the absorbed dose is delivered more acutely. As $T \to \infty$, then $G \to 0$. A plot of G as a function of the product of the repair constant and irradiation time is shown in Fig. 10.24.

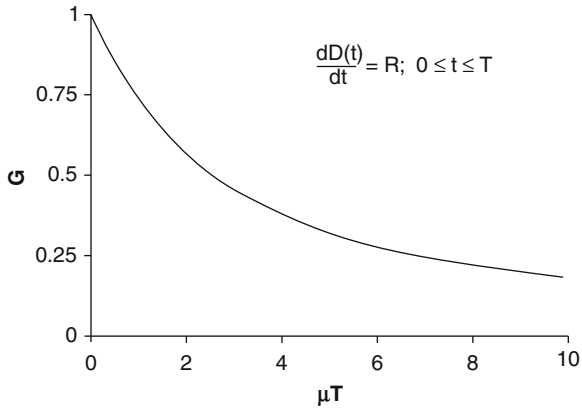

Fig. 10.24 Lea–Catcheside dose-prolongation factor G as a function of the product of μT for a constant absorbed dose rate for a finite time T and where μ is the first-order repair rate constant

Exponentially-Decreasing Absorbed Dose Rate

For an example more representative of nuclear medicine, consider the Lea–Catcheside factor for an exponentially-decreasing absorbed dose rate,

$$\begin{aligned} \frac{dD(t)}{dt} &= Re^{-\lambda t} \quad 0 \leq t \leq T \\ &= 0 \quad \text{elsewhere.} \end{aligned} \tag{10.26}$$

For calculational purposes, a finite irradiation time has been allowed for, whereas in internally-administered absorbed dose, $T \to \infty$. The total absorbed dose is,

$$\begin{aligned} D &= \int_{-\infty}^{\infty} dt \frac{dD(t)}{dt} \\ &= R \int_0^T dt \, e^{-\lambda t} \\ &= \frac{R}{\lambda} \left(1 - e^{-\lambda T} \right). \end{aligned} \tag{10.27}$$

The Lea–Catcheside factor for this particular absorbed dose rate model is given by the evaluation of the double integrals,

$$
\begin{aligned}
G &= \frac{2}{D^2}\int_{-\infty}^{\infty} dt \frac{dD(t)}{dt}\int_{-\infty}^{t} dt' \frac{dD(t')}{dt'} e^{-\mu(t-t')} \\
&= 2\left(\frac{R}{D}\right)^2 \int_0^T dt\, e^{-\lambda t}\int_{-\infty}^{t} dt'\, e^{-\lambda t'}\, e^{-\mu(t-t')} \\
&= 2\left(\frac{\lambda}{(1-e^{-\lambda T})}\right)^2 \int_0^T dt\, e^{-(\lambda+\mu)t}\int_{-\infty}^{t} dt'\, e^{-(\lambda-\mu)t'} \\
&= \frac{2}{\lambda-\mu}\left(\frac{\lambda}{(1-e^{-\lambda T})}\right)^2 \int_0^T dt\, e^{-(\lambda+\mu)t}\left(1-e^{-(\lambda-\mu)t}\right) \\
&= \frac{2}{\lambda-\mu}\left(\frac{\lambda}{(1-e^{-\lambda T})}\right)^2 \left(\frac{1-e^{-(\lambda+\mu)t}}{\lambda+\mu} - \frac{1-e^{-2\lambda T}}{2\lambda}\right)
\end{aligned}
\tag{10.28}
$$

By again expanding the exponentials of (10.28) to second order, it is seen, after some algebraic manipulation, that the dose-protraction factor $G \to 1$ as $T \to 0$. For nuclear medicine dosimetry, one would want to calculate G_∞, which is the value for G as $T \to \infty$ and $t \to \infty$,

$$G_\infty = \frac{\lambda}{\lambda+\mu} \tag{10.29}$$

This G_∞ term is plotted in Fig. 10.25 as a function of the ratio of the decay to repair constants, λ/μ. From this figure, $G_\infty \to 1$ as $\lambda/\mu \to \infty$.

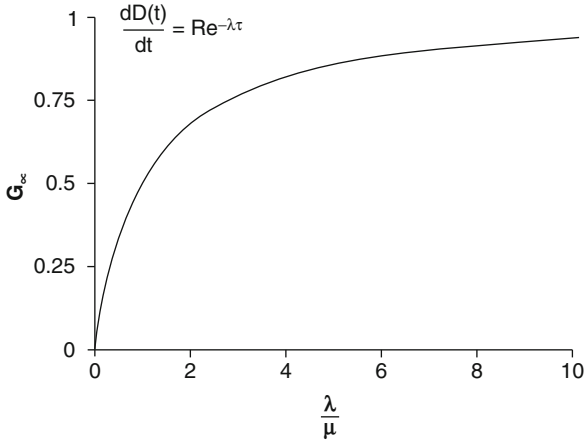

Fig. 10.25 Lea–Catcheside dose-protraction factor at infinite time for exponentially-decreasing absorbed dose rate as a function of the ratio of the effective decay constant (accounting for both physical decay and biological washout) to the repair time constant, λ/μ

The absorbed dose rate to a given tissue as a result of the administration of a radionuclide generally does not follow a simple monoexponential decrease It takes a finite amount of time for the tissue to uptake the radionuclide and the biokinetics are frequently such that washout follows a multiexponential temporal behavior. The Lea–Catcheside factor can be calculated by modeling the absorbed dose as a superposition of weighted exponential terms and calculating each separately and the final result obtained by the weighted summation of terms.

10.3.3 Biologically Equivalent Dose

From (10.14), the logarithm of the fraction of cells of a population that has been irradiated to an absorbed dose D is given as,

$$-\ln S = \alpha D + \beta G D^2 \tag{10.30}$$

The negative logarithm of the fractional survival is replaced by defining it as the biological effect of interest, $E \equiv -\ln S$. For a single acute absorbed dose given over a time duration much less than that time required for repair, we can then set the Lea–Catcheside factor $G = 1$ and the biological effect as,

$$E = \alpha D + \beta D^2. \tag{10.31}$$

Now, consider the case if the same net absorbed dose is administered but now expended over n fractions so as to enable damage repair between fractions. As the absorbed dose per fraction is $d = D/n$, the biological effect for fractionated radiotherapy is,

$$
\begin{aligned}
E &= n\left(\alpha d + \beta d^2\right) \\
&= \alpha n d\left(1 + \frac{d}{\alpha/\beta}\right) \\
&= \alpha D\left(1 + \frac{d}{\alpha/\beta}\right).
\end{aligned}
\tag{10.32}
$$

Dividing through by α gives,

$$BED = D\left(1 + \frac{d}{\alpha/\beta}\right). \tag{10.33}$$

$\mathrm{BED} \equiv \mathrm{E}/\alpha$ is the biologically equivalent dose[6] and is equal to the product of the total absorbed dose and the factor $\left(1 + \frac{\mathrm{d}}{\alpha/\beta}\right)$. This latter factor is itself known as the relative effectiveness, RE, so that the definition of the BED can be written as,

$$\mathrm{BED} = \mathrm{D} \times \mathrm{RE}. \tag{10.34}$$

The relative effectiveness for a constant absorbed dose rate R for time T is,

$$\mathrm{RE} = 1 + \frac{\mathrm{R}(\mu\mathrm{T} + \mathrm{e}^{-\mu\mathrm{T}} - 1)}{\mu^2\,\mathrm{T}\,\alpha/\beta} \tag{10.35}$$

For the case of the continuous and exponentially-decreasing absorbed dose rate of (10.26),

$$\mathrm{BED} = \mathrm{D}\left(1 + \frac{\mathrm{G}_\infty \mathrm{R}}{\lambda\left(\alpha/\beta\right)}\right). \tag{10.36}$$

Hence,

$$\mathrm{BED} = \frac{\mathrm{R}}{\lambda} \times \mathrm{RE} \tag{10.37}$$

and the relative effectiveness is,

$$\mathrm{RE} = 1 + \frac{\mathrm{R}}{(\lambda + \mu)\left(\alpha/\beta\right)} \tag{10.38}$$

It would be useful at this point to employ an example to describe a practical use of these results. Consider the case of a tumor (with the ratio $\alpha/\beta = 10\,\mathrm{Gy}$ and repair constant $\mu = 0.5\mathrm{h}^{-1}$) to be treated with ^{131}I through internal administration. The effective half-life of the radionuclide in the tumor, accounting for both the biological washout and the physical decay of the isotope, is taken to be 5 days (i.e., $\lambda = 0.006\mathrm{h}^{-1}$). One wishes to determine the initial absorbed dose rate required with the radionuclide therapy using ^{131}I so as to achieve the total absorbed dose required to achieve the same biological effect as if the tumor had been treated to a total absorbed dose of 50 Gy over a period of 5 days using a ^{137}Cs source. As the half-life of ^{137}Cs is far greater than the 5-day treatment time, we can treat it as a source of radiation providing a constant absorbed dose rate of 0.417 Gy/h to the tumor. Using (10.33), the biologically equivalent dose is 58.2 Gy. Substituting (10.34) into (10.37) and solving for the absorbed dose rate R from ^{131}I administered internally for this value of the BED, R = 0.324 Gy/h. The resulting total absorbed dose from the ^{131}I radionuclide therapy is 54 Gy, which is the absorbed dose required to yield the same biological effect upon the tumor as delivering 50 Gy to it continuously over 5 days by a ^{137}Cs source. Further discussion in relation to applications to the medical internal radiation dose (MIRD) schema can be found in Baechler et al. (2008).

[6]Also referred to as the extrapolated response dose (Wheldon and O'Donoghue 1990) or as the biologically effective dose.

10.3.4 Effects of Repopulation

The above derivations neglected cell population growth in order to simplify the various derivations. But, in reality, cells within a population (e.g., a tumor) can proliferate during and following irradiation which will result in a reduction of the BED (Dale 1996). This effect can be accounted for, admittedly crudely, by modifying the expression for the biologically effective dose to include a reductive factor in (10.37),

$$\mathrm{BED} = \frac{\mathrm{R}}{\lambda} \times \mathrm{RE} - \frac{\ln 2}{\alpha}\frac{\mathrm{t}}{\mathrm{T}_{\mathrm{Pot}}} \tag{10.39}$$

where it has been assumed that the clonogens increase exponentially over time t and where $\mathrm{T}_{\mathrm{Pot}}$ is defined to be the potential doubling time of the cell population. Hence, the ratio $\mathrm{t}/\mathrm{T}_{\mathrm{Pot}}$ gives the number of cell doublings during t.

10.3.5 Applications of the Linear-Quadratic Model to Internal Radiation Dosimetry

10.3.5.1 Introduction

The applications of the LQ model to address problems in internal radiation dosimetry began with the seminal paper by Dale (1985).

10.3.5.2 α/β Ratios

Recall that the α/β ratio is the absorbed dose at which the linear and quadratic contributions to the biological effect are equal. Thus, in terms of the description offered by the cell survival curve, the curve will be shallower and more slowly bending for cells with high α/β ratios and correspondingly steeper and more curved for cells with low α/β ratios. In general, late reacting tissues are slowly dividing and have low α/β ratios of the order of 3 Gy or so. Acutely-reacting tissues, which are more rapidly dividing (such as neoplasia, skin, and intestinal epithelium), have higher α/β ratios, with values typically about 10 Gy.

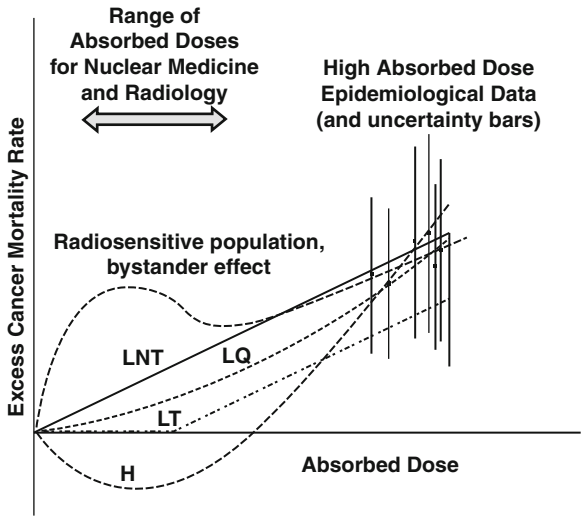

Fig. 10.26 Conceptual representation of the extrapolation of epidemiological dose–response data of ECMR from high absorbed doses to the low absorbed doses typical of medical imaging procedures. Five extrapolation models are shown: linear no threshold (LNT), linear threshold (LT), linear-quadratic (LQ), hormesis (H), and a bimodal model which predicts an elevated risk at low doses due to, for example, the bystander effect

10.4 Human Somatic Effects of Ionizing Radiation

10.4.1 Introduction

Cellular radiobiology enables both the estimation of the probability of cellular death or mutation as a consequence of exposure to ionizing radiation and the study of various influencing effects such as hypoxia and absorbed dose rate. While investigations of irradiated cells or colonies of cells are fundamental to understanding both the risks posed by ionizing radiation and how these risks can be modified or mitigated against, extrapolation of these cellular data to the metazoan level in order to predict unequivocally the effects of ionizing radiation upon the human is not possible. Consequently, the estimations of risk and effect resulting from medical exposures to ionizing radiation are reliant upon the experiences of exposures of human populations to ionizing radiation. In particular, because radiation-induced mutations and their consequences are no different than those that occur spontaneously or through other insults (e.g., chemical or viral), the effects of ionizing radiations at the low absorbed doses associated with medical imaging are assessed through epidemiological studies in which large cohorts of irradiated individuals are compared with large unirradiated populations in order to observe statistically the elevated incidence of a mutation or its effect resulting from ionizing radiation. These epidemiological sources are the subject of the following subsection.

A significant problem in estimating radiation risk is that many of these sources of human radiation exposure data are for absorbed doses that are much greater than those typical of medical diagnostic exposures. In order to use these data (e.g., elevated risk of cancer per unit absorbed dose) to estimate the risk to the patient receiving much lower doses, cellular radiobiology can be called upon to guide the development of dose–response models that can extrapolate from high absorbed dose epidemiological risks to those at the low absorbed doses associated with medical diagnostic procedures, including nuclear medicine. Figure 10.26 presents the difficulty of estimating the risk associated with the low absorbed doses due to medical imaging exposures (here, the risk is the excess cancer mortality rate (ECMR) beyond that observed in a population unexposed to radiation[7]) by using the risks determined through epidemiological studies at higher absorbed doses. Although these latter risks are subject to bias and confounding and are determined by

[7]Such a condition is hardly achievable as all populations are exposed to at least background radiation. Hence, the control population would be that that was not exposed to the test radiation.

comparing a population exposed to known absorbed doses against another matched unexposed population. Ideal matching must be in terms of age, sex, race, and exposure to other confounding carcinogens such as tobacco. Clearly, this isolation and matching of cohorts is difficult to achieve. Moreover, the uncertainty bars associated with the determined risk values are inherently large. Even assuming that perfect statistical matching of the populations is obtained, the observed risks must then be extrapolated to the low absorbed doses of interest accounting for the effects of absorbed dose rate, the LET of the radiation creating the absorbed dose and the above noted characteristics of the exposed and unexposed populations. Clearly, this is not a trivial problem to address and the interested reader is advised to consult, for example, the BEIR V and BEIR VII reports (National Research Council 1990, 2006) for a full exposition of the practicalities. What is of interest is, following from the earlier review of radiobiology, are the different types of radiobiological models used to extrapolate from the absorbed doses of the measured data to the range of absorbed doses of interest to us so as to provide an estimate of the risk associated with a diagnostic nuclear medicine study. Clearly, the first requirement of the extrapolation model is that it be able to reproduce the observed risks at higher absorbed doses and to then "sensibly" extrapolate to the low absorbed doses of interest to us. Radiobiology can guide the selection of an appropriate model. As a result, different estimates of risks at the absorbed dose range of clinical interest occur.

Five dose–response models for the ECMR are presented in Fig. 10.26.

Linear no threshold (LNT) response: This is the simplest dose-risk model in which the risk is considered to be proportional to absorbed dose,

$$\text{ECMR} = \alpha_{\text{LNT}}\, \text{D} \tag{10.40}$$

where D is the absorbed dose and α_{LNT} is a constant of proportionality. This model predicts that there is *always* an excess risk of cancer induction and mortality as a function of dose and is only zero (i.e., equal to that which "naturally" occurs) at zero absorbed dose. This is perhaps the basic dose–response model in that it assumes that ionizing radiation produces irrepairable DNA lesions and that repair is neglected.

Linear threshold (LT) response: This dose–response model is a variant of the LT model, Here, the effect of sublethal cellular repair is accounted for in a simplistic fashion in that the model assumes that there is no risk of excess cancer mortality below some absorbed dose threshold, D_{T},

$$\begin{aligned} \text{ECMR} &= 0 \qquad \text{D} \le \text{D}_{\text{T}} \\ &= \alpha_{\text{LT}}\, \text{D} \quad \text{D} > \text{D}_{\text{T}}. \end{aligned} \tag{10.41}$$

Our understanding of the repair of sublethal and potentially lethal damages does not account for the existence of a threshold absorbed dose, D_{T}, below which stochastic radiation damage cannot occur. This requires more involved appreciations of the effects of the absorbed dose rate, times between fractionated radiation exposures and environmental conditions. Hence, this is a simplistic model which implies that, at absorbed doses less than D_{T}, individual cells can repair radiation damage or, somatically, the body can eradicate any nascent tumors through, for example, an immunological response.

LQ response: From the earlier discussion of the LQ model, it is possible to hypothesize that the risk behaves in the form,

$$\text{ECMR} = \alpha_{\text{LQ}}\, \text{D} + \beta_{\text{LQ}}\, \text{D}^2 \tag{10.42}$$

where the first term describes the effects of fatal DSBs and the quadratic term describes the effects of secondary DSBs. The Lea–Catcheside factor describing sublethal repair of initial DSBs is not included in this expression.

Hormetic (H) response: This is a controversial dose–response model in which it is assumed that the exposure to very low absorbed doses of radiation triggers an immunological response sufficient to eliminate any neoplasms. As a result, the cancer risk of the irradiated population is lower than that of a corresponding unirradiated population. This effect then reverses with increasing absorbed dose to present a risk that increases with absorbed dose (Luckey 1991).

Bystander response: It has been described how the bystander effect can lead to an elevated response at low absorbed doses. Should this model be valid, then there would be an increase in risk response at lower absorbed doses. However, such an effect would be difficult to discern in nuclear medicine due to the

distribution of radioactivity within the body (Sgouros et al. 2007).

It is difficult to select from these models one that is appropriate for predicting effects at low absorbed doses and which is what would be regarded as a "reasonable" extrapolation from epidemiological data. For the purposes of the protection of the patient, the radiation worker or any other individual exposed to ionizing radiation, the most conservative model linking risk to absorbed dose is the LNT model. It is currently regarded that the scientific arguments and supporting epidemiological data for the use of the LT, LQ, bystander, and hormetic models in radiation protection are insufficient to cause abandonment of the LNT model. Hence, the use of the LNT model in radiation protection is still recommended in both International Commission on Radiological Protection (ICRP) Publication 103 (ICRP 2007) and the BEIR VII report of the National Academy of Sciences. This recommendation is, however, most certainly not without controversy. Whereas most epidemiological studies suggest that there is no evidence for cancer induction at effective doses (to be defined later) below about 150 mSv, which is 10–40 times greater than that received in most diagnostic nuclear medicine procedures, there has been indications that effective doses as low as even 10 mSv, which is of the order of magnitude of most diagnostic nuclear medicine studies, can be associated with the induction of solid tumors (Brenner and Hall 2007).

10.4.2 Epidemiological Sources of Human Data

Observations of the effects of ionizing radiation upon individual cells are insufficient to predict somatic effects. Inevitably, though, an understanding of the potential risk posed by exposure to ionizing radiation can only be obtained from analyses of populations of individuals exposed to ionizing radiation.

10.4.2.1 Nuclear Bombings of Hiroshima and Nagasaki

The largest cohort of individuals exposed to ionizing radiation is that of the survivors of the nuclear bombings of Hiroshima and Nagasaki at the end of the Second World War. The life span study (LSS) population consists of 120,321 individuals who were resident in those two cities in 1950, of whom 91,228 were present at the times of the detonations. This population has been followed up since that date. The population present at the detonations was made up of two subcohorts: one made up of survivors who were within 2.5 km of the detonations' hypocenters and a similar-sized control group who were between 3 and 10 km from the hypocenters and who received negligible absorbed doses.

This population presents three significant advantages in minimizing bias in estimating the risks resulting from exposure to ionizing radiation. First, it is a large heterogeneous population in terms of age and sex. Second, no bias is introduced in terms of disease (as in long-term survivors of radiotherapy) and occupation (as in radiation workers). Third, exposures were of the whole body enabling the assessment and comparison of cancer risks at different anatomical sites. However, there were a number of significant difficulties in estimating the absorbed doses received by individuals that were not resolved until 1980s (Radiation Effects Research 1987a, b; National Research Council 1990). The fissioning of both weapons produced neutrons and γ rays. Neutrons elastically scatter from protons in tissue and the secondary protons, due to their mass, present a high-LET radiation compared to the Compton electrons and photoelectrons set in motion by the γ rays. As Fig. 10.15 indicates, the LET-dependence of biological effects requires a clear separation of the contributions of neutrons and photons to the absorbed dose received in order to isolate their biological effects. The neutron fluences of both weapons differed because of their designs.[8] Earlier estimates of the neutron and photon absorbed doses grossly overestimated that due to neutrons due to, among other things, not allowing for attenuation of the neutron fluence by the water content (i.e., protons) of the humid air. The neutron and photon fluences have been estimated by Monte Carlo simulations, postdetonation measurements using neutron- and

[8]The "Little Boy" weapon used at Hiroshima consisted of two subcritical masses of ^{235}U, one of which was fired into the other to form a critical mass which subsequently fissioned. The "Fat Man" weapon used at Nagasaki consisted of a subcritical spherical mass of ^{239}Pu which was imploded to form the critical mass.

photon-emitting sources, and in situ measurements such as thermoluminescent dosimetry of building materials exposed to the blasts. Another factor of importance in being able to apply the survivor data (excess cancer incidence or mortality per unit absorbed dose) to provide risk estimates is that the exposure was essentially instantaneous. Recall that the incidence of a biological effect for a given fixed dose increases with dose rate. This, plus consideration of the extrapolation to low absorbed doses, requires that the application of the bomb survivor data incorporates a dose and dose-rate effectiveness factor (DDREF) to correct for the prompt exposure and arrive at a risk estimate more appropriate to protracted exposure to low absorbed doses. Figure 10.27 demonstrates how this factor was obtained in the BEIR VII report. The value of the DDREF is 2, but it is recognized that there is considerable uncertainty associated with this value (ICRP 2007).

There, however, remain two major complicating factors to be accounted for. First, during the conditions of war at the time, the Japanese population were malnourished and their intrinsic susceptibility to the effects of ionizing radiation could have been elevated thus increasing the estimates of risk per unit absorbed dose. The second, and countering effect, is that of the "healthy survivor." This effect predicts that the survivor had a predisposition to surviving prior to exposure to radiation and, as a result, would tend to decrease the estimate of risk per unit absorbed dose.

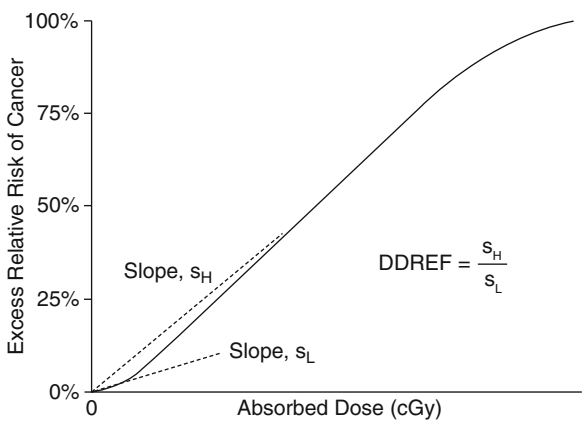

Fig. 10.27 The rationale for the dose and dose-rate effectiveness factor (DDREF) defined in the BEIR VII (2006) report for a hypothetical dose–response curve. A linear approximation at low absorbed doses (i.e., the tangent to the curve at zero absorbed dose) yields the slope s_L. At higher absorbed doses, where the response is linear, an extrapolated slope s_H is obtained. The DDREF is the ratio of these two slopes

10.4.2.2 Medical Exposures: Examples

Retrospective analyses of cancer incidence in patient populations who have undergone medical exposures to ionizing radiation have, in general, the advantages of consistent and extended follow-up periods and the availability of accurate dosimetry data. Unfortunately, these populations can introduce a significant bias as a result of the disease for which they have been exposed to ionizing radiation.

There are two groups of medically-exposed subjects to be considered. The first is that made up of long-term surviving radiation oncology patients. Here, the exposed tissues and organs of interest are not those within the treatment portal, which receive a tumoricidal absorbed dose, but rather those extraneous to it and which receive only scattered radiation and much lower absorbed doses. Clearly, the requirement of the subjects to have survived for an extended period (beyond the latency period in order for a radiogenic cancer to be manifest) limits such cohorts to specific cancers and radiotherapy regimes with high survival probabilities. These include, for example, cancers of the cervix and breast and Hodgkin's disease (lymphoma). The second group is that of patients that have undergone diagnostic imaging procedures. While the magnitude of the absorbed doses received by this latter population are typical of those of interest to our application to nuclear medicine, it is generally far more difficult to retrospectively estimate the absorbed dose in these patients than for the therapeutic patients.

Secondary Neoplasia in Radiotherapy Patients

Patients suffering from cancers are frequently treated with ionizing radiation with curative intent; in fact, about half of all oncology patients receive radiotherapy during the course of treatment of their disease (Ron 1998). Radiotherapy is performed predominantly with X-rays or high-energy electrons produced by linear accelerators or γ rays from a radioisotope source (e.g., ^{60}Co, ^{137}Cs). Proton irradiation is growing as a means of therapy, particularly in the United States of

America, and, historically, pions and heavy ions have been used. Those patients with long survival times can express secondary tumors attributable to the therapeutic ionizing radiation they have received. These secondary malignancies can occur in regions outside the primary therapy portal (within which the radiation absorbed dose would have been intended to tumoricidal, with absorbed doses of the order of 50 Gy and greater) due to radiation scattered from the irradiated volume or from leakage radiation emitted by the treatment device. The magnitudes of the absorbed doses in these peripheral regions can be similar to those experienced in diagnostic imaging procedures and the detailed radiation prescriptions and treatment plans allow accurate retrospective estimation of doses at such sites. Even so, as the doses of interest for estimating the radiation risk associated with diagnostic levels of absorbed dose are of the order of tens of mGy compared to the therapeutic absorbed doses of tens Gy, accurate measurement, or calculation of such peripheral doses for radiotherapy patients receiving high absorbed doses within the treatment portal is challenging and frequently necessary (McParland and Fair 1992; Stovall et al. 1995).

Three populations of long-term surviving oncology patients treated with radiation have provided the most abundant data.

Cervical cancer: Long-term survivors treated for cervical cancer have provided a significant cohort to assess radiocarcinogenesis as a result of exposure to low absorbed doses. Radiotherapy is provided through intracavitary ^{137}Cs sources[9] within the cervix and/or uterus or external radiation beam therapy to give high absorbed doses to the cervix and uterus (several tens of Gy). Peripheral tissues will also receive a radiation absorbed dose due to the Compton scattering of photons from the treatment volume. Absorbed doses to the active bone marrow has been estimated to be as high as 7 Gy; absorbed doses to the breast and lung tissue are estimated to be of the order of 300 mGy and that to the thyroid is estimated to be 100 mGy (Kleinerman et al. 1995). Epidemiological studies by Boice et al. (1985) and extended by Kleinerman et al. were conducted for up to some 7,543 secondary cancers resulting from about 200,000 cervical cancer patients reviewed in eight countries. Specific details of the elevated risks of secondary cancers in these long-term survivors can be found in the original publications or in the BEIR V and VII reports.

Hodgkin's disease: Another cohort of long-term radiotherapy survivors are those treated by radiation for Hodgkin's disease. This is a lymphoma predominantly of younger populations and is frequently treated successfully with radiation, usually in conjunction with chemotherapy. As a result of its extended shape and location, the primary radiation portal is referred to as the "mantle field" due to its encompassing the axillary, mediastinal, and cervical lymph nodes. Additional radiation portals can be used to irradiate the spleen and Waldeyer's ring. This combination of a young age and a long survival time lends well to follow-up studies of secondary cancers attributable to scattered radiation received by tissues peripheral to the primary radiation field. In particular, the extended radiation field leads to the investigation of secondary cancers such as leukemia and solid cancers of the breast and lung.

Breast cancer: Long-term survivors of breast cancer treated with radiation provide yet another cohort of subjects at risk to secondary cancers attributable to the therapeutic radiation field. Lung cancer, leukemia, and contralateral breast cancer have been studied as sequelae due to radiotherapy of primary breast cancer with retrospective dose estimation derivable from measurement (McParland 1990).

Radiation therapy has also been used for benign conditions, of which three significant cohorts providing data of radiation-induced cancer risk are summarized.

Ankylosing spondylitis: This is a chronic arthritis affecting the spine and sacroiliac joints. Between 1935 and 1957, radiotherapy was used in the United Kingdom for the treatment of this disease. A cohort of 14,566 patients received spinal irradiation and was followed up into the 1990s (Weiss et al. 1994); the radiation dosimetry was estimated by Monte Carlo simulations of a sample of patients. The cancer mortality rate amongst the irradiated patients was significantly greater than those expected from rates in England and Wales, with significant increases seen in leukemia, non-Hodgkin's lymphoma, multiple myeloma, and solid tumors of the esophagus, pancreas, lung, urinary bladder wall, and kidney.

[9] In much earlier times during the twentieth century, ^{226}Ra sources were used. These were largely supplanted by safer ^{137}Cs sources in the 1970s and 1980s.

Tinea capitis: This is a fungal infection of the scalp and the use of X-rays to epilate the scalp was a frequent means of treating the infection. For example, between 1948 and 1960 in Israel, approximately 20,000 children were treated in such a manner (Ron et al. 1998). Epidemiological studies of children irradiated for tinea capitis revealed elevated incidences of brain tumors (glioblastoma and meningioma); a follow-up of 2,215 patients was performed for 25 years postirradiation (Shore et al. 1976).

Postpartum mastitis: Prior to the introduction of antibiotics and sulfonamides, irradiation was a frequent mode of treatment for inflammatory conditions. Some 601 women between 20 and 40 years of age were treated with radiation in the state of New York for postpartum mastitis during the 1940s and 1950s and received absorbed doses to breast tissue between 60 cGy and 14 Gy and exposures. This exposed cohort was compared against 1,239 women suffering from the same condition but who did not receive radiotherapy.

Cancers Arising from Diagnostic Imaging Procedures

Assessing the elevated risks of radiation-induced cancers from patient cohorts exposed to ionizing radiation in diagnostic imaging procedures can be difficult as accurate retrospective assessment of the absorbed dose and the anatomical sites being imaged is not as easy to achieve as with patients receiving therapeutic exposures. On the other hand, the sizes of populations undergoing diagnostic procedures are greater than those undergoing therapy and do not have the confounding factor of differentiating between "naturally-occurring" and radiation-induced secondary cancers arising in a patient having demonstrated a predisposition to malignancy. Moreover, they received absorbed doses with approximately the same magnitude for which one wishes to assess the risks associated with imaging. This latter point is a double-edged sword: although the low magnitudes of absorbed doses are comparable to the problem at hand, the concurrent reduction in cancer risk requires greater population sizes in order to derive a statistically-valid estimate of cancer risk per unit absorbed dose.

Fluoroscopy-aided artificial pneumothrax in treatment of pulmonary tuberculosis: A theoretical approach to treating patients suffering from pulmonary tuberculosis developed in the nineteenth century was to induce an artificial pneumothorax allowing drainage of the pleural space and cicatrization of pulmonary injuries. Beginning in the early part of the twentieth century, this therapeutic technique was coupled with fluoroscopic review which led to large numbers of patients being exposed to X-irradiation. Three epidemiological studies following up women having received multiple fluoroscopies in conjunction with artificial pneumothorax have provided significant data on radiation risk associated with the exposure of certain organs. The first consists of 31,710 women in Canada who received fluoroscopy-associated artificial pneumothorax therapy between 1930 and 1952, with many receiving multiple fluoroscopies with wide ranges of fractionations (e.g., BEIR VII reports a mean number of 92 fluoroscopy-aided artificial pneumothorax procedures per patient over periods of up to 2 years). Of this population, 8,380 received an absorbed dose to the breast exceeding 10 cGy (with a maximum exceeding 2 Gy). Of particular interest is the fact that patients in the Canadian province of Nova Scotia were generally imaged in the anterioposterior view (i.e., the X-rays incident to the patient's anterior) whereas the posterior–anterior view was prevalent elsewhere. The former patients would clearly receive a much higher absorbed dose to the breast.

Thorium-based vascular contrast medium: The radiation exposure of interest here is not that from the external X-ray beam, but rather that due to the radioactive thorium used in the vascular contrast. Thorotrast was a vascular contrast agent consisting of ThO_2 in a colloidal suspension used in the 1930s and 1940s. Thorium was selected for this application due to its high atomic number ($Z = 90$) and consequent high photoelectric absorption cross section allowing visualization of the vasculature in X-ray imaging. However, its dominant isotope is ^{232}Th which is an α emitter with a half-life of 14.1×10^9 years; the α particle has a kinetic energy of 4.1 MeV. There is a high uptake of the ^{232}Th by the liver, spleen, and bone. Liver washout is especially slow and in excess of 20 years. Follow-up studies in Europe, Japan, and the United States of America of those patients receiving Thorotrast have been conducted. In such studies, the absorbed dose to the liver from the α particles was estimated to be as high as 2 Gy and

elevated incidences of angiosarcomas, biliary duct carcinomas, and hepatocellular carcinomas with a risk of the order of 3×10^{-2}/man-Gy for a latency period of 20 years.

In utero exposures: Of particular practical clinical nuclear medicine interest is the risk to the irradiated embryo or fetus. As proliferative cells are more radiosensitive than those that are not, the risk to the irradiated in utero being is expected to be elevated and, thus, of obvious concern. This has a specific clinical bearing as the leading risk of death during pregnancy is pulmonary embolism (PE) thus requiring imaging through either CT perfusion angiography or ventilation–perfusion scintigraphy, both of which contribute a radiation dose to the fetus. The Oxford Survey of Childhood Cancers (Stewart et al. 1956, 1958) and its reanalysis by Bithell and Stiller (1988) and a study conducted in the state of New England in the United States of America (MacMahon 1962) investigated the incidence of childhood cancer following in utero irradiation from diagnostic X-rays. The latter was extended to consider cancer mortality amongst 1,429,400 American children and demonstrated an excess in cancer incidence in those irradiated with X-rays in utero.

10.4.2.3 Occupational Exposures

Miners

One cohort exposed to radiation in the course of their occupation was miners. These individuals were chronically exposed to α particles resulting from the radioactive decays of ^{222}Rn and ^{226}Rn which are isotopes of radon which is an inert gas and a daughter product of ^{226}Ra.

Radiologists

The comparison of the cancer mortality rate of radiologists with those of other medical practitioners is based upon the expectation that radiologists practicing in the early part of the twentieth century were more likely to have received higher radiation absorbed doses due to then-primitive radiation protection practices than other physicians or radiologists who practiced in the latter part of the twentieth century.

Berrington et al. (2001) reported on an analysis of the causes of death of 2,690 radiologists registered in the United Kingdom and Ireland between 1897 and 1997 which found increased cancer mortality amongst radiologists registered up to 1954 compared to other physicians. After that year, there was no difference in the cancer mortality risks of radiologists and other physicians. The discussion, however, of radiologist risk has not been without debate and further examination (Cameron 2002; Doll et al. 2005).

Nuclear Workers

These cohorts are made up of individuals working in the civilian nuclear power industry and in shipyards building and servicing nuclear-propelled vessels such as submarines. A study of in excess of 95,000 workers in the United Kingdom, United States of America, and Canada demonstrated no excess risk in solid tumors, but a slight excess in leukemia in the United Kingdom cohorts was observed (Hall and Giaccia 2006).

Radium Dial Painters

This is perhaps the best-known cohort of individuals exposed to radiation through their occupation. These were workers who painted dials of watches and clocks with a radium-containing paint that fluoresced and was visible in the dark. They were predominantly women and who frequently shaped the paint brush with their lips, thus ingesting ^{226}Ra. Elevated incidences of osteosarcomas were observed (as there is high uptake of radium by bone) and of carcinomas in the paranasal sinuses and mastoid air cells, the latter presumably due to the radon gas product of the radium decay.

10.4.2.4 Chernobyl

The greatest recognized population accidentally exposed to ionizing radiation were those individuals living in the vicinity of the Chernobyl nuclear power reactor at the time of its explosion and of the firefighters sent to the site. Many of the latter suffered high radiation exposures and died, despite attempts at salvage through bone marrow transplantation, of symptoms reflective of the GI syndrome described in

the following subsection. Of particular interests in the former population were the incidences of thyroid cancers due to the release of the fission product ^{131}I into the environment.

10.4.3 Radiation Pathologies

10.4.3.1 Introduction

Exposure of the whole body, or of specific sensitive organs or tissues, to high absorbed doses can culminate in acute effects leading to death. In diagnostic nuclear medicine, this acute radiation syndrome is not reached due to the very low amounts of administered activity and the consequent low organ absorbed doses. This is often not the case in therapeutic nuclear medicine where the radiotoxicities of red bone marrow (which leads to the hematopoietic syndrome) and kidney (leading to nephrotoxicity) can often limit the amount of administered activity.

Most data of the effects of total-body exposure to high absorbed doses of radiation are derived from animal experiments; human data are limited primarily to experiences of radiotherapy patients, the survivors of the Hiroshima and Nagasaki nuclear bombings and accidental exposures. Hall and Giaccia (2006) report that throughout the world some 120 fatalities resulted from radiation exposures arising from accidents involving radioactive material occurring between 1944 and 1999.

For a given population, the percentage of mortalities as a function of absorbed dose follows a sigmoidal curve, as shown in Fig. 10.28. The median lethal dose, labeled as LD_{50}, is about 400 cGy for humans (in the absence of therapy, such as bone marrow salvage).

Immediately following the exposure of a large part of the body to an absorbed dose exceeding the order of 50 cGy, early transitory symptoms appear. At absorbed doses comparable to the LD_{50} value given above, the resulting symptoms of irradiation include anorexia, nausea, and vomiting. At supralethal absorbed doses, the symptoms include diarrhea and hypotension, referred to as the prodromal radiation syndrome. This prodromal reaction is followed by a largely asymptomatic latent period, the duration of which is largely dictated by the kinetics of cell depletion in the irradiated tissues; an exception to this is the cerebrovascular syndrome for

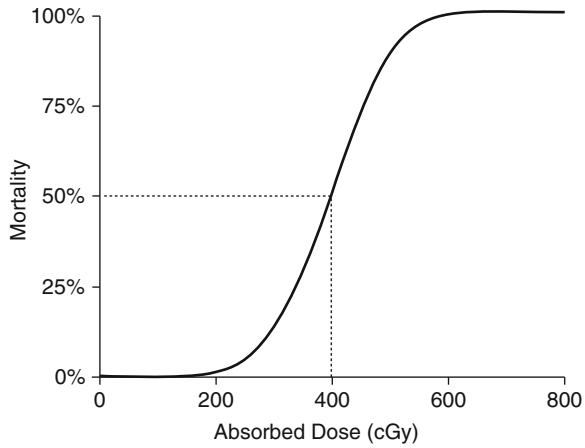

Fig. 10.28 A sigmoidal curve describing the mortality-absorbed dose relationship without salvage. The LD_{50} for the human is about 400 cGy

which the onset of death is rapid. Hematologic aplasia can be evident at absorbed doses as low as 50 cGy with a decrease in circulating lymphocyte counts.

10.4.3.2 Cerebrovascular Syndrome

A whole-body dose of the order of 50–100 Gy will result in death within 48 h of exposure.[10] While all organ systems will be severely damaged as a result of such an irradiation, cerebrovascular damage brings death so rapidly that these other organ system effects cannot be manifested. The exact cause of death from the cerebrovascular syndrome is not clear. It has been typically attributed to cerebral edema, with extravasation of fluid, macrophages, and granulocytes into the brain and meninges. However, this description may not present the complete case as much higher absorbed doses are required to bring on this syndrome should only the brain be irradiated.

10.4.3.3 Gastrointestinal Syndrome

At whole-body absorbed doses of the order of 10 Gy, cells in the epithelial lining of the GI tract are

[10] In these discussions, we assume that the exposure is to photons (X or γ rays); due to the high-LET of the resulting recoil protons, the biological effects can be achieved at lower absorbed doses of neutrons.

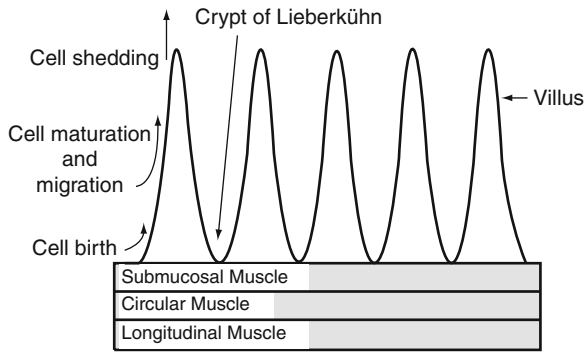

Fig. 10.29 Diagrammatic representation of the intestinal wall

depleted. The organization of this lining is that of self-renewing tissue. The mucosal walls of the intestine are covered by villi (as shown diagrammatically in Fig. 10.29) at a density of 20–40 villi/mm^2 and each villus projects about 0.5–1 mm and is covered by a single layer of columnar epithelium. The mucosa of the intestinal villi can be divided into four compartments. The stem cell compartment is at the base of the villus (the crypt of Lieberkühn) which is a region of great mitotic activity. Progressing up the villus, the cell differentiating compartment is found which also has a high mitotic index: this produces the functional cells which are found at the tip of the villus. Finally, at the villus' tip, the spent functional cells are sloughed off into the intestinal lumen.

Following irradiation to absorbed doses of about 10 Gy, the crypt and differentiating cells are killed off but the extrusion of the functional cells from the villi tips continues. As the villi surfaces are sloughed off due to the normal transit of material through the intestines, the villi begin to contract and, due to the non-replacement of the extruded cells, breaches of the intestinal lining occur in regions of denuded intestine leading to infection by intestinal flora. The presentation of denuded intestinal wall occurs a few days postirradiation in the human and the distal end of the irradiated small intestine is unable to resorb bile salts which enter the large intestine causing irritation and diarrhea. Because the magnitude of the absorbed dose will also lead to the individual being immunocompromised, any infections that occur within the intestinal wall can spread. Death in the human can subsequently occurs within a few days following irradiation.

10.4.3.4 Hematopoietic Syndrome

Whereas the cerebrovascular and GI syndromes are associated with high absorbed doses that are presented only in extreme circumstances, the hematopoietic syndrome can occur for absorbed doses comparable to those experienced in radiotherapy. Indeed, this syndrome presents the barrier of radiotoxicity to many approaches of radionuclide therapy. For absorbed doses of between 2.5 and 5 Gy, mitotically-active stem cells are killed off and the supply of erythrocytes and leukocytes is markedly diminished. The pathology resulting from the exposure to radiation does not occur until a number of weeks later when the circulating mature blood cells die off and the precursor cell supply is compromised.

10.4.4 Deterministic (Non-Stochastic) Effects

10.4.4.1 Introduction

This subsection reviews determinisitic effects associated with lower absorbed doses than those linked to the pathologies of the cerebrovascular, GI, or hematopoietic syndromes. The absorbed doses required to induce such pathologies are not typical of diagnostic medical procedures, although the radiotoxicity associated with the hematopoietic syndrome is a dose-limiting factor in therapeutic nuclear medicine. A deterministic effect is defined as a radiation effect in which there is an absorbed dose threshold of expression. Below this absorbed dose, there is no manifestation of an effect; but once this threshold is breached, the pathology becomes apparent and the degree of severity of the effect increases with absorbed dose, as shown in Fig. 10.30. Because of variations between individuals, the absorbed dose threshold is highly variably over a population. Table 10.3 summarizes absorbed dose levels at which such effects can become apparent.

10.4.4.2 Erythema and Epilation

These effects are observed in radiation therapy due to the high absorbed doses involved. They are, however,

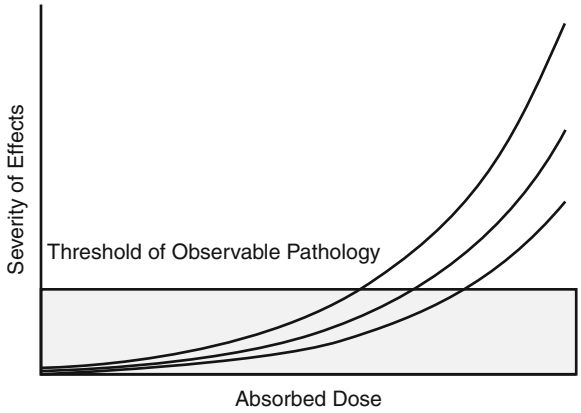

Fig. 10.30 Typical dose–response curves for a deterministic effect. Below a threshold, there is no observable pathology but, beyond which, the severity of the effect becomes manifest and increases with absorbed dose. The absorbed dose at which this effect is apparent varies among individuals as demonstrated by the three curves

Table 10.3 Absorbed dose thresholds for a selection of deterministic effects

Deterministic effect		Approximate typical threshold absorbed dose for acute exposure (Gy) (50% incidence in 5 years postirradiation)
Bone marrow: aplasia		0.5
Liver: hepatitis		40
Brain: infarction and necrosis		70
Lung: pneumonitis		35
Kidney: nephrosclerosis		25
Sterility	Female: permanent	60
	Male: temporary	0.15
	Male: permanent	50

not associated with either diagnostic or therapeutic nuclear medicine, but have been associated with some extreme forms of diagnostic exposures received in fluoroscopy examinations.

10.4.4.3 Sterilization

The effects of ionizing radiation upon individual germ cells have been described previously. Because of the difference between male and female gonadal kinetics, the induction of sterility differs between male and female in terms of degree and absorbed dose. The absorbed dose thresholds for temporary and permanent sterility are summarized in Table 10.3

10.4.4.4 Cataractogenesis

A cataract is any change in the transparency of the lens and it has long been recognized that exposure of the eye to ionizing radiation can result in the induction of a cataract. Cataractogenesis has been detected in both patient and medical practitioner as a result of diagnostic imaging irradiation. As protracted exposures require absorbed doses exceeding 5 Gy to the lens of the eye in order to induce a cataract, this effect is highly unlikely to result from a nuclear medicine procedure. However, it can be a potential risk associated with irradiation of the eye in diagnostic procedures such as cranial CT or fluoroscopy.

10.4.5 Stochastic Effects

10.4.5.1 Introduction

Stochastic effects are those for which the severity of outcome is independent of radiation dose but the probability of occurrence increases with absorbed dose. For example, consider a case of two women both exposed to ionizing radiation but from which one receives a higher absorbed dose to the breast than the other. The probability of breast cancer induction in the woman receiving the lower absorbed dose is expected to be less than that of the woman receiving the higher absorbed dose. However, the consequences of either morbidity or mortality are equal should both cancers be expressed in either woman, regardless of the probability of cancer induction. The stochastic effects resulting from exposure to ionizing radiation of interest are carcinogenesis and hereditary effects. Ionizing radiation does not lead to new stochastic effects attributable to radiation alone: all that can occur is the increase in the probability of the occurrence of deleterious effects which are manifested naturally.

There are two simple categories of epidemiological models which describe the elevation in risk resulting from exposure to ionizing radiation. The first is the absolute risk model in which exposure to ionizing

radiation additively increases the incidence rate above the naturally-occurring rate. The second is the relative risk model in which the implicit assumption is that ionizing radiation merely increases the natural risk at all ages of exposure by a given factor. For the example of cancer, as the natural incidence of cancers increases with age, the relative risk model emphasizes a greater degree of radiocarcinogenesis in old age. A preferred modification of the relative risk model is to incorporate a time dependence. For example, let λ be the rate of cancer mortality of an irradiated population (e.g., the number of cancer deaths per unit population exposed to radiation) and λ_0 be that rate in an unirradiated population.

The epidemiological definition of the excess absolute risk (EAR) of cancer mortality is defined as

$$\mathrm{EAR} = \lambda - \lambda_0. \tag{10.43}$$

The relative risk of cancer mortality is,

$$\mathrm{RR} = \frac{\lambda}{\lambda_0} \tag{10.44}$$

and the excess relative risk (ERR) is, combining the above two results,

$$\begin{aligned} \mathrm{ERR} &= \frac{\lambda - \lambda_0}{\lambda_0} \\ &= \mathrm{RR} - 1. \end{aligned} \tag{10.45}$$

Note that both the relative and the ERRs are dimensionless quantities.

10.4.5.2 Radiation Carcinogenesis

The incidence of cancer following the exposure to low absorbed doses of ionizing radiation is of obvious concern to diagnostic nuclear medicine. This subsection considers the risks of three specific radiogenic cancers: leukemia, female breast, and thyroid. Models derived from epidemiological data and presented in the BEIR VII report are used in this subsection and considered in the context of low-LET radiation typical of diagnostic nuclear medicine. The risk is typically a function of the sex of the individual, the age at which exposure occurred, the age for which the risk is evaluated (i.e., time postexposure) and the absorbed dose received by the tissue of interest.

Leukemia

Radiation-induced leukemia was the first cancer to have been linked to the radiation exposures received by the survivors of the nuclear bombing of Hiroshima and Nagasaki (indeed, as from the deaths of many of the pioneers of the radiation sciences, such as Marie Curie). Moreover, it is recognized as being the cancer with the highest relative risk following exposure to ionizing radiation and is thus deserving of investigation. The BEIR VII parametric model of the ERR of radiation-induced leukemia is a function of absorbed dose, age of exposure, and of elapsed time following exposure. The sex-specific model of the ERR is,

$$\mathrm{ERR} = \beta\, \mathrm{D}(1 + \theta \mathrm{D}) \mathrm{e}^{(\gamma \varepsilon^* + \delta \ln \mathrm{t}/25 + \phi \varepsilon^* \ln \mathrm{t}/25)} \tag{10.46}$$

where, for the consideration here of photon and electron radiation, D is the absorbed dose to the marrow (i.e., we need not consider the equivalent dose) and the mean estimated parameters are,

$$\begin{aligned} \beta &= 1.1\,\mathrm{Gy}^{-1} && \text{Male} \\ &= 1.2\,\mathrm{Gy}^{-1} && \text{Female;} \end{aligned}$$

$$\begin{aligned} \varepsilon^* &= \frac{\varepsilon - 30}{10} && \varepsilon \le 30 \\ &= 0 && \varepsilon > 30 \end{aligned}$$

where ε is the age at the time of exposure and the further parameters are,

$\gamma = -0.40$ per decade
$\delta = -0.48$
$\phi = 0.42$
$\theta = 0.87\ \mathrm{Gy}^{-1}$.

t is the time postexposure in units of years. Figure 10.31 shows a plot of the example of the ERR per Gy for a female 20 years of age at the time of exposure as a function of time following exposure,

The ERR per unit absorbed dose is elevated at early times postexposure, eventually subsiding to unity at about 45 years postexposure.

Breast Cancer

As the incidence of breast cancer incidence will vary with culture, diet, etc., most calculations of the ERR for radiogenic breast cancer are frequently referenced

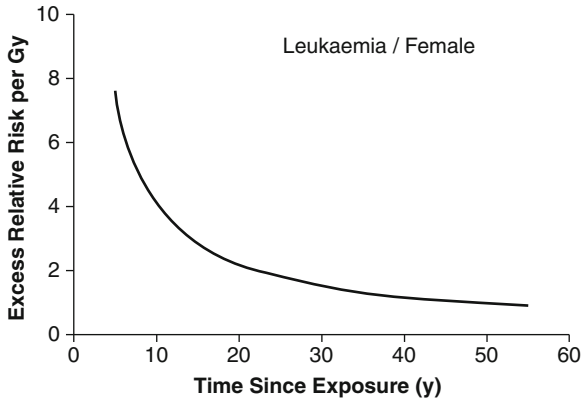

Fig. 10.31 Predicted ERR per Gy of leukemia for a 20-year-old female exposed to low-LET radiation as a function of time postexposure. Curve is calculated using (10.46) and mean values of parameters given in the BEIR VII report

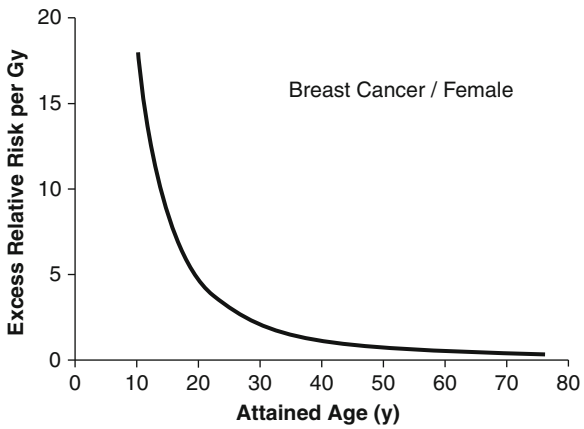

Fig. 10.32 Predicted ERR per Gy of breast cancer in the female as a function of attained age calculated from (10.47)

to North American women. Assuming, again, low-LET radiation, the ERR of breast cancer above the naturally-occurring rate, per Gy is modeled by the function in age,

$$\mathrm{ERR} = 0.51\left(\frac{60}{\mathrm{A}}\right)^2 \mathrm{Gy}^{-1} \tag{10.47}$$

where A is the attained age in years. This ERR is shown in Fig. 10.32 as a function of attained age.

Thyroid Cancer

The induction of thyroid cancer as a result of the exposure of the thyroid gland to radiation due to, for example, the high levels of radioactive iodine uptake by the population of the Marshall Islands who were subject to the radioactive fallout of the BRAVO thermonuclear bomb test in 1954 and those exposed to the radioactive fallout of the Chernobyl accident in 1986, is well quantified. For low-LET radiation, the BEIR VII model of thyroid cancer incidence as a function of age at the time of exposure is,

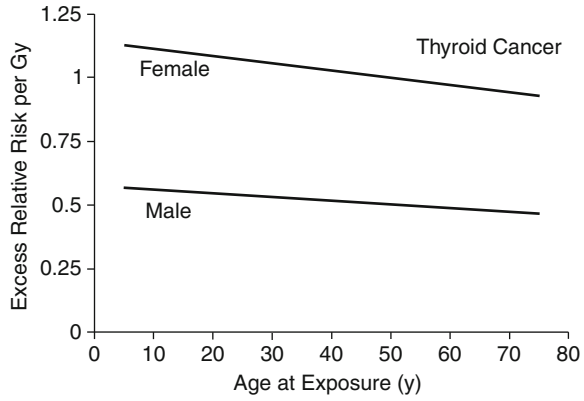

Fig. 10.33 Excess relative risk per unit absorbed dose of thyroid cancer incidence for males and females as a function of the age at exposure derived from the BEIR VII model

$$\mathrm{ERR} = \beta \mathrm{e}^{-0.083\left(\frac{\varepsilon-30}{30}\right)} \tag{10.48}$$

where $\beta = 0.53$ for males, $\beta = 1.05$ for females and where ε is the age (in years) at the time of exposure. It should be recalled that ERR is multiplied by the naturally-occurring rate of thyroid cancer incidence to give the increased incidence due to ionizing radiation. This ERR as a function of the age at exposure is shown in Fig. 10.33.

It is immediately obvious that females are subject to a greater risk of radiogenic thyroid cancer than are males.

10.4.5.3 Hereditary Effects

Radiation-induced mutations in germ cells can lead to hereditary effects passed on to the progeny of the exposed individual. Such mutations do not lead to new or unique mutations that are specific to ionizing radiation. Hence, a convenient metric of quantifying the hereditary effects of ionizing radiation is through

the "doubling dose," which is the absorbed dose required to increase the natural frequency of an hereditary effect by a factor of two. An estimate of the average doubling dose for low-LET radiation is 1.56 Gy (Hall and Giaccia 2006), whereas ICRP Publication 103 assumes the incidence of genetic risks up to the second generation following exposure to ionizing radiation as 0.2%/Gy over continuous low-dose rate exposure. Because of the naturally-occurring rate of hereditary effects, it is difficult to detect any radiation-induced mutations appearing in the progeny of irradiated individuals. In fact, to quote ICRP Publication 103: "There continues to be no direct evidence that exposure of parents to radiation leads to excess heritable disease in offspring" and that reports lend to the argument "...that the risk of heritable diseases tended to be overestimated in the past." Even so, prudence is necessary in assigning risks to hereditary effects occurring as a result of exposure to ionizing radiation. This is a consequence not necessarily of the risk itself but of its consequences. To explain this, one should consider the fact that a radiation-induced cancer can only affect the individual exposed. In the worst outcome, only a single individual dies. But in the case of a radiation-induced mutations passed onto the irradiated individual's offspring, a potentially deleterious mutation will have been inserted into the gene pool and more than just the irradiated individual can be affected. Hence, even though the risk of heritable disease as a consequence of exposure to ionizing radiation has not been demonstrated in the human, a risk coefficient for such effects is assigned.

10.5 Antenatal Effects

10.5.1 Introduction

Irradiation of the embryo and fetus is known to result in effects which may be manifest in either prenatal or neonatal states and which are dependent upon absorbed dose, gestational age, and absorbed dose rate. Recognizing that rapidly differentiating cells are more prone to radiation-induced damage, it is not unexpected that the embryo and fetus are acutely sensitive to the effects of ionizing radiation.

Medical irradiation of the pregnant patient is always of concern and presents the clinician of the starkest requirement of the optimization of risk and benefit of medical exposure to ionizing radiation. For example, most medical physicists practicing in nuclear medicine have been confronted with a case of a female patient in late pregnancy requiring a ventilation–perfusion scan to rule out PE, a condition which is the most important preventable cause of maternal death and with an incidence reaching 1.3% of all pregnancies (Chan and Ginsberg 1999). The need to estimate the absorbed dose to the fetus resulting from this procedure and contrasting the theoretical radiation-induced risk with the risks of failing to diagnose a present PE or the sequelae associated with the administration of an anticoagulant is almost always required in such situations. This subsection reviews the demonstrated risks of the result of maternal irradiation and the dose–response of these risks.

Prenatal sensitivity to ionizing radiation varies remarkably over the time of fertilization to implantation and gestation. During each cycle, within the ovarian cortex, a Graffian follicle containing a mature ovum moves to the surface of the ovary which ruptures to release the ovum into an awaiting end of the Fallopian tube which is likely brought into proximity of the ovary by chemotaxis. This process is known as ovulation. Once within the lumen of the Fallopian tube, the ovum is transported towards the uterus through ciliary action and peristalsis. Fertilization typically occurs shortly after intercourse (within 3 h) in the ampullary section of the Fallopian tube. The fertilized ovum is now a zygote and arrives at the uterus within about 5 days of fertilization. Whilst the zygote is still within the Fallopian tube, it begins to divide to form a mass of cells referred to as the morula, within which a cavity appears and the structure forms a blastocyst. Once the blastocyst has reached the uterus, it becomes embedded within the endometrium and extravasation of the maternal blood occurs around the blastocyst to provide its nutrition through maternofetal exchange. This description of the trail from ovulation to implantation and prenatal development is necessary for understanding the radiation sensitivities of the zygote, blastocyst, embryo, and fetus, and our characterizations of the risks. Following the use of Russell and Russell (1954), we simplify the discussion by dividing the prenatal phase into three components:

Preimplantation: That period of time (5–6 days) between fertilization in the Fallopian tube and the embedding of the blastocyst in the endometrium

Organogenesis: That period of time following implantation during which the major organs develop

Fetal period: That period of time during which the developed organs grow

10.5.2 Embryonic Death

Irradiation of the embryo can result in death. Absorbed doses of the order of 2–3 Gy delivered to the embryo in the first 20 days of gestation are likely to result in the resorption of the embryonic material or abortion of the embryo.

10.5.3 Microcephaly and Mental Retardation

Severe injuries to the developing human brain were documented in the survivors of the Hiroshima and Nagasaki bombings. The gestational age at which exposure occurred is critical to understanding the radiation-induced damage. Four categories of gestational age are aligned to development of the brain: 0–7 weeks, 8–15, 16–25, and greater than 26 weeks. The precursors of the neuroglia and neurons appear and are mitotically active during the first gestational stage which is followed by the second gestational stage which is marked by an increase in the number of neurons and their migration to their developmental sites subsequent to their cessation in mitotic capacity. During the third stage, synaptogenesis accelerates and the cytoarchitecture of the developing brain has been defined. Further advancements in cytoarchitecture differentiation and synaptogenesis occur in the final stage of gestational development.

The sensitivity of the developing brain is thus expected to be dependent upon the in utero absorbed dose and gestational age. Most of the epidemiological data to derive these results were obtained from children exposed in utero at the Hiroshima and Nagasaki bombings and the consequences of irradiation were microcephaly and mental retardation. Microcephaly is associated with in utero exposures at less than 15 weeks gestational age without an apparent threshold absorbed dose. The incidence of mental retardation is linearly related to the fetal absorbed dose during the critical gestational age of 8–15 weeks with an incidence risk coefficient of about 40%/Gy and which is commensurate with an absorbed dose threshold of about 15 cGy. Absorbed doses of such magnitudes are unachievable in diagnostic nuclear medicine.

10.5.4 Childhood Cancer

Childhood cancer as a consequence of in utero irradiation was recognized in studies of children irradiated in utero from radiological obstetric examinations and the Hiroshima and Nagasaki bombings. The sensitivity of childhood neoplasia due to prenatal irradiation peaks during the third trimester of pregnancy (Bithell and Stiller 1988). The EAR is estimated to be about 5%/Gy. In practical terms, ICRP Publication 103 (ICRP 2007) advises that the lifetime risk of cancer as a consequence of in utero exposure is no different from exposure during early childhood which is no more than three times that of the general population.

10.6 Radiation Risks Presented to the Diagnostic Nuclear Medicine Patient

10.6.1 Introduction

Consideration of the safety of the diagnostic nuclear medicine patient will clearly emphasize stochastic effects as deterministic effects of exposure to ionizing radiation are unachievable due to the low absorbed doses received by such a patient. Consequently, the foci of discussion will be on radiocarcinogenesis (of either the patient or the fetus should the patient be pregnant) and the potential for hereditary effects.

The fundamental problem in translating the risks determined from epidemiological studies to those of the diagnostic nuclear medicine patient is that both the subjects in the source data cohorts and the patient are, in general, irradiated nonuniformly. Different organs and different tissues have differing

radiosensitivities, as demonstrated earlier in the ERRs of the breast, thyroid gland, and leukemia. As a result, the simple use of the physical quantity of absorbed dose is inadequate to derive the risk an individual is subject to as a result of nonuniform irradiation. Moreover, consideration must be taken of the sex and age of the individual and the time elapsed since exposure. It is immediately apparent that the mapping from the simple physical description of absorbed dose to an assessment of stochastic risk is highly complicated.

The ICRP has addressed these problems since the 1970s with simple, applicable and generic solutions which are periodically refined through the incorporation of new knowledge of the effects of ionizing radiation. These account for, first, the physical attributes of the radiation that the individual is exposed to (e.g., LET and absorbed dose rate) and, second, the inherent radiosensitivity of the individual organs and tissues irradiated. This latter consideration includes dependencies (which are averaged) upon sex, age, and absorbed dose rate. As a result, one must reflect upon the effective dose as a quantity which is rather unspecific and best suited as a means of comparing the relative risks between differing types of radiation exposure.

10.6.2 ICRP Recommendations

The ICRP publishes recommendations on radiation protection which is updated about every 5–15 years (ICRP 1959, 1964, 1966, 1977, 1991, 2007). The three publications of most modern-day relevance are those of Publication 26 (ICRP 1977), which was superseded by Publication 60 (ICRP 1991) which has been superseded, in turn, by Publication 103 (ICRP 2007).

Of particular importance to those imaging procedures incurring low doses of ionizing radiation, the ICRP has defined the quantity of the effective dose as a sex-, age-, and dose rate-independent measure of the stochastic risk presented to an individual as a result of a nonuniform irradiation. Note that this quantity is applicable to stochastic risk only. The ICRP Recommendations equate the stochastic risk of nonuniform radiation (of high- and/or low-LET radiation) to that resulting from uniform (i.e., total body) exposure: in other words, the effective dose due to nonuniform irradiation is numerically equal to the absorbed dose from a whole-body exposure to low-LET radiation that yields the same stochastic risk.

10.6.3 Equivalent (Radiation Weighted) Dose

10.6.3.1 Introduction

The ICRP Recommendations consider radiological protection in a wide variety of applications including medical (both practitioner and patient), occupational, and aviation exposures. As a result these must account for several different species of radiations: photons, electrons/positrons, neutrons, protons, α particles, and pions (the latter being a component of cosmic rays and consequently of interest to radiation exposure associated with high-altitude aviation). Following from the discussions of Chaps. 6 and 7, it will be recognized that these radiations will have different LETs resulting in, as shown earlier in this chapter, different RBEs. These are accounted for by defining the equivalent dose which is the absorbed dose weighted by a factor, w_R, to account approximately for the RBE relevant to the radiation of interest. For nuclear medicine dosimetry, these are photons and electrons/positrons resulting from β decay (α particle and Auger/Coster–Kronig electrons are relevant only to therapeutic applications associated with high absorbed doses).

10.6.3.2 Radiation Weighting Factor, w_R

The equivalent dose to a given tissue or organ is the weighted summation of the absorbed doses to that tissue or organ T from all of the radiations that it is exposed to,

$$H_T = \sum_R w_R D_{T,R} \tag{10.49}$$

where w_R is the radiation weighting factor for radiation species R and $D_{T,R}$ is the corresponding (physical) absorbed dose to the tissue from that radiation. The

Table 10.4 Radiation weighting factors used in ICRP Publications 26, 60, and 103

Radiation	Radiation weighting factor, wR		
	ICRP Publication 26 (1977)	ICRP Publication 60 (1991)	ICRP Publication 103 (ICRP, 2007)
γ, $e^{\pm}$, $\mu^{\pm}$ (excluding Auger electrons)	1	1	1
Protons	10	2	2
$\pi^{\pm}$	–	–	2
α particles, fission fragments, heavy nuclei	–	20	20
Neutrons	10	Function of neutron energy	Function of neutron energy

radiation weighting factor is an approximation of the LET of the radiation. The radiation weighting factors provided by ICRP Publications 26, 60, and 103 are provided in Table 10.4

The absorbed dose is averaged over the entire organ and the physical unit of the equivalent dose is that of the absorbed dose, Gy, but, because the quantity is committee-defined, is assigned the special name sievert (Sv).

As the weighting factor for photons and electrons/positrons[11] is unity, one can interpret the equivalent dose of a given combination of radiations to an organ or tissue as being equal to the (physical) absorbed dose in photons or electrons (with $w_R = 1$) that yields the same biological effect to the individual organ.

Auger/Coster–Kronig electrons are treated by the ICRP as a special case in which it is recognized that it is inappropriate to average the absorbed doses from these radiations over the total mass of DNA should such electron-emitting isotopes be incorporated within the DNA. If the Auger/Coster–Kronig electron-emitting isotope is external to the cell, the efficiency of producing any biological effect is negligible due to the very short ranges of Auger electrons. However, should the radionuclide be incorporated within the nucleus, the RBE increases. If Auger electrons are emitted from within the cell, but not from within the nucleus, the RBE can be as high as 8 (Kassis et al. 1988). For cases where the Auger electron-emitting radionuclide is incorporated within the nucleus and, subsequently, the DNA, RBE values in excess of 20 have been measured. The ICRP states that the biological effects of Auger electrons are omitted from the radiation weighting factors of Table 10.4 and must be dealt with using microdosimetry.

[11]Excluding Auger/Coster–Kronig electrons.

10.6.4 Effective Dose

10.6.4.1 Introduction

Medical radiation protection practice must contend with two important facts. First, almost all medical radiation exposures are nonuniform throughout the body and, second, tissues and organs have varying radiosensitivities. Thus, in order to estimate the stochastic risk associated with a given imaging study, one must know which organs/tissues have been irradiated, the equivalent doses received by them and their intrinsic radiosensitivities. Determining the absorbed doses received by organs and tissues in nuclear medicine is the fundamental topic of the following chapter. The intrinsic radiosensitivities are derived from the data described earlier in this chapter. The contribution of these to an overall estimate of radiation risk is modeled by the tissue weighting factor, w_T.

10.6.4.2 Tissue Weighting Factor, w_T

The effective dose is the sum of the equivalent doses over a defined ensemble of organs and tissues each weighted by a tissue weighting factor,

$$E = \sum_T w_T H_T \tag{10.50}$$

In ICRP 26, this tissue weighting factor reflected only mortality risk whereas in ICRP 60 and ICRP 103 it reflected a quantity known as detriment which is an aggregate of four quantities:

- Probability of attributable fatal cancer
- Weighted probability of attributable nonfatal cancer

- Weighted probability of severe hereditary effects
- Relative amount of time of life lost

In ICRP 26, the weighted equivalent dose, which is a doubly-weighted absorbed dose, was assigned the name effective dose equivalent. The tissues and organs considered in the calculation of the effective dose have grown over the three publications reflecting the expanding knowledge of the radiosensitivities of these tissues. Table 10.5 summarizes the historical development of the weighting factors provided by ICRP Publications 26, 60, and 103.

The procedure recommended in ICRP Publication 103 of calculating the effective dose on the basis of the measured biodistribution of a radionuclide is shown in Fig. 10.34. The biodistribution is used to calculate the absorbed doses to specified tissues and organs of reference male and female anthropomorphic phantoms. The application of the radiation weighting factors converts these absorbed dose quantities to equivalent doses for each specified tissue and organ. Having calculated the equivalent doses, these are then averaged to yield an ensemble of organ and tissue equivalent doses for the male and female reference phantoms. These are then further averaged over both sexes to yield a single ensemble of tissue equivalent doses and the tissue weighting factors are then applied to yield the effective dose.

Table 10.5 Tissue weighting factors used in ICRP Publications 26, 60, and 103

Tissue or organ	Tissue weighting factor, w_T		
	ICRP Publication 26 (1977)	ICRP Publication 60 (1991)	ICRP Publication 103 (2007)
Brain	–	–	0.01
Salivary glands	–	–	0.01
Red bone marrow	0.12	0.12	0.12
Lung	0.12	0.12	0.12
Breast	0.15	0.05	0.12
Colon wall	–	0.12	0.12
Stomach wall	–	0.12	0.12
Esophagus	–	0.05	0.04
Bone surface	0.03	0.01	0.01
Skin	–	0.01	0.01
Thyroid gland	0.03	0.05	0.04
Gonads	0.25	0.20	0.08
Liver	–	0.05	0.04
Urinary bladder wall	–	0.05	0.04
Remaining tissues	0.30[a]	0.05[b]	0.12[c]

[a]The remaining tissues in ICRP 26 are the stomach, salivary glands, lower large intestine wall, and liver

[b]The remaining tissues in ICRP 60 are the adrenal glands, brain, upper large intestine wall, small intestine wall, kidney, muscle, pancreas, spleen, thymus, and uterus. Further modifications were recommended in later ICRP publications and are discussed in the text

[c]The remaining tissues in ICRP 103 are adipose tissue, adrenal glands, connective tissue, extrathoracic airways, gallbladder wall, kidneys, cardiac wall, lymphatic nodes, muscle, pancreas, prostate gland, small intestine wall, spleen, thymus, and uterus/cervix

Table 10.5 is an excellent example of displaying how the understanding of the effects of radiation dosimetry has evolved over the decades. For example, the most profound change has been the weighting factor assigned to the absorbed dose to the gonads which has decreased from 0.25 in ICRP Publication 26 to 0.20 in ICRP Publication 60 and, finally, to 0.08 in ICRP Publication 103. These reductions reflect the recognition over time that radiation-induced hereditary effects are much less likely than had been previously believed.

In diagnostic medicine, one is interested in a measure of the risks associated with the nonuniform exposure to low-dose ionizing radiation. The ICRP has provided estimates of the detriment per unit effective dose in both Publications 60 and 103. These are summarized in Table 10.6 (as the recommendations of these publications are applicable to those who are occupationally exposed to ionizing radiation, risk factors are calculated separately for adult workers and the general population, the latter including children).

The most marked change in stochastic risks between those specified by ICRP 60 and 103 is that assigned to severe hereditary effects. Any change in hereditary effects due to exposure ionizing radiation is measured by comparing the incidence of these effects in an irradiated population with a matched nonirradiated population. This reflects that the natural incidence of these effects in the natural (nonirradiated) population is not that markedly lower than that of the appearance of these effects in the matched irradiated population.

10.6.4.3 Additional Considerations

Following the release of ICRP Publication 60, the ICRP has published a number of refinements to the evaluation of the effective dose.

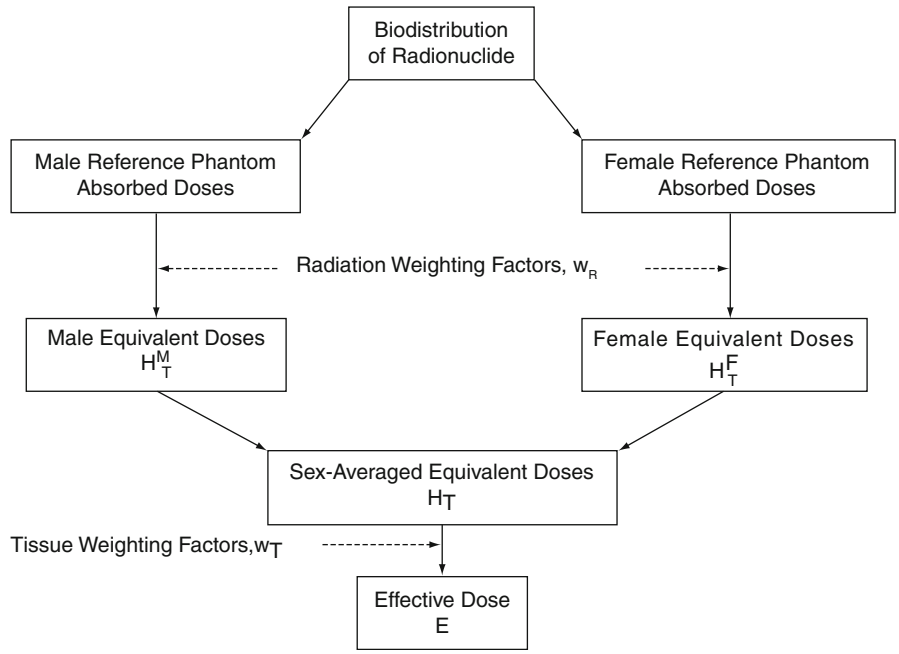

Fig. 10.34 Means of estimating the effective dose following the recommendations of ICRP Publication 103

Table 10.6 Nominal probability coefficients for stochastic effects from ICRP Publications 60 and 103

Exposed populations		Detriment (Sv^{-1})			
		Fatal cancer	Nonfatal cancer	Severe hereditary effects (%)	Total
Adult workers	ICRP 60	4.0%	0.8%	0.8	5.6
	ICRP 103	4.1% (combined)		0.1	4.2
Entire population	ICRP 60	5.0%	1.0%	1.3	7.3
	ICRP 103	5.5% (combined)		0.2	5.7

Gonadal Absorbed Dose

As the individual for whom the effective dose is often to be calculated for is an adult hermaphrodite, in such a case the absorbed doses to the gonads are to be averaged over the testicular and ovarian absorbed doses.

Esophagus/Thymus Absorbed Dose

The esophagus is a specified organ in the evaluation of the effective dose. However, the esophageal absorbed dose is not calculated for in the MIRD schema used in nuclear medicine (Chap. 11). To resolve this discrepancy, the absorbed dose to the thymus is used as a surrogate to that to the esophagus.

Colon Absorbed Dose

For radiation dosimetry purposes, the anatomy of the colon is considered to consist of:

- The ascending colon which is defined as being the extent of the bowel from the cecum to the hepatic flexure.
- The transverse colon which is defined as extending between the hepatic and splenic flexures.
- The descending colon which extends from the splenic flexure and includes the sigmoid colon and the rectum.

In ICRP Publication 60, the upper large intestine (ULI) wall is included within the remaining tissues category. However, the ICRP later recommended an alteration to the manner in which the absorbed dose to the walls of the colon and the corresponding tissue

weighting factors contribution to E were to be evaluated. The absorbed dose to the colon is to be given by the mass-weighted absorbed doses to the walls of the ULI and lower large intestine (LLI),

$$D_{Colon} = 0.57\, D_{ULI} + 0.43\, D_{LLI}. \tag{10.51}$$

The ULI is defined as that portion of the colon from the cecum, the ascending colon to the hepatic flexure; the transverse colon is that from the hepatic flexure to the splenic flexure; and, the LLI consists of the descending colon from the splenic flexure, the sigmoid colon, and the rectum.

10.6.4.4 Use of the Effective Dose in Nuclear Medicine

The use of the effective dose as a descriptor of radiation risk arising from medical exposures has long been contentious (e.g., Martin 2007; Brenner 2008; Dietze et al. 2009). This has been largely a consequence of the multiple acts of averaging over sex and age and the simplification of the biological effects of absorbed dose rate when using epidemiological data. Further, the effective dose does not account for the dependence of risk upon age at exposure and the tissue weighting factor represents a detriment, which is an amalgam of the endpoints of cancer mortality and incidence, hereditary risk, and reduction in life expectancy. Martin (2007) has suggested the means of how the effective dose should be used in assessing or comparing the risks associated with medical exposures. His key recommendation is that the use of the effective dose be simply as a generic indicator or risk to a reference hermaphroditic phantom. More specific risk estimates for a given patient should following the organ-, sex-, and age-specific risk models, examples of which were provided earlier.

10.7 Radiobiology Considerations for the Therapeutic Nuclear Medicine Patient

10.7.1 Introduction

Whereas the intent of the application of radiobiology to the diagnostic nuclear medicine patient is for estimating the potential for stochastic risk resulting from the exposure to low doses of low-LET radiation, the corresponding application to the therapeutic patient is markedly different. As noted several times before, biological effect in therapeutic nuclear medicine is sought in terms of killing tumor cells, whilst minimizing radiation-induced damage to normal tissue. This balance between tumor control probability (TCP) and radiotoxicity, or normal tissue complication probability (NTCP), is critical to the curative intent of therapeutic nuclear medicine.

10.7.2 Tumor Control Probability

One can consider that there are two endpoints for tumor response, those of sterilization and remission. Thus, tumor control is, as would be evident, related to the number of remnant viable tumor cells. Applying Poisson statistics, one can define the TCP as,

$$TCP = e^{-N_t} \tag{10.52}$$

where N_t is the number of surviving clonogenic tumor cells.

10.7.3 Normal Tissue Complication Probability

The NTCP is not only a function of the physical attributes of irradiation (LET and absorbed dose rate[12]), but also a function of the tissue's organizational structure. Normal tissue tolerance is the result of the ability of the clonogenic cells of the tissue to ensure an adequate number of mature cells required to enable normal organ or tissue function to continue. But this is also subject to the hierarchical structure of the tissue, hence the previous emphasis on mature cells. Rapidly proliferating stem cells are, as discussed earlier, sensitive to radiation. These stem cells differentiate to eventually produce functional cells which are less sensitive to radiation. Examples of this

[12]For external beam radiotherapy, the fractionation regime must also be considered.

hierarchical model are hematopoietic bone marrow and the intestinal epithelium. The resulting effects of radiation upon these tissues have a latent period: the pluripotential stem cells are killed off more readily by irradiation, but, due to the serial time development of the tissue, this is not apparent in terms of organ function until the mature cells have been depleted and there are no replacements from the descendants of the now-depleted stem cells.

Other tissues do not exhibit such a hierarchical structure, an example being the liver. Normally, the cells of such tissue rarely undergo mitosis but can be induced to do so following trauma or injury to the tissue. The tissue structure lacks a hierarchy and, as a result, all cells begin to divide following an insult.

Many organs or tissues may be considered to be made up of functional subunits (FSUs) which can be discrete and clearly defined structures contributing to the function of the organ and tissue. An example is the nephron in the kidney. The exchange of clonogenic cells between FSUs is not possible. In some tissues, the FSUs are not so clearly defined; examples include mucosa and the skin. Differentiation between the two types of FSU categorization is important as the responses to radiation differ between them. Due to each FSU being independent and small, depletion of the cells within it can be readily achieved through low absorbed doses. This, for example, explains the relatively low radiation tolerance of the kidney. On the other hand, migration of cells between structurally undefined FSUs is possible: an area of skin denuded due to radiation can be restored by the transfer of clonogenic cells from surrounding unaffected skin.

Tolerance doses are frequently quantified by $TD_{5/5}$ and $TD_{50/5}$ which are the tolerance doses yielding a 5% complication rate in 5 years and a 50% complication rate in 5 years, respectively. Values for these tolerance doses are, in general, derived from external beam radiotherapy and, hence, are complex functions of fractionation, absorbed dose rate, and fraction of the volume of organ/tissue irradiated. Meredith et al. (2008) provide a comparison of tolerance dose between external beam radiotherapy and radionuclide therapy using β-emitting radionuclides.

The tolerance doses of normal tissues will clearly vary between tissues and, indeed, between patients. For radionuclide therapy, the normal tissue which defines the radiotoxic limit is frequently the active bone marrow which would be recognized as having a tolerance dose of a few hundred cGy.

Meredith et al. (2008) have summarized the three main points associated with normal tissue tolerance to radionuclide therapy:

- The tolerance of normal tissue is affected by absorbed dose rate.
- The inhomogeneous distribution of absorbed dose affects the tolerance of the irradiated organ as a whole.
- The FSUs of different organs (e.g., kidney and spinal cord) have different tolerances.

Wessels et al. (2008) have recently shown how radiobiology concepts can be incorporated within the MIRD schema for estimating the risk of normal tissue complications to the kidney.

10.7.4 Selection of Isotopes for Radionuclide Therapy

The selection of a particular isotope for radionuclide therapy must consider several biological, chemical, and physical factors which can be distilled into three categories:

Radiation quality: For radiotherapy, particulate radiations (α particles, β particle, and Auger/Coster–Kronig electrons) are best suited due to the limited range and high LET of the particles. The limited ranges of these particles are advantageous in that this can limit radiotoxicity by reducing the absorbed doses to normal, healthy tissues provided that the vector carrying the radioisotope has a high specificity for the target. Kassis (2003) has noted the implication of the differences between the LET of α emitters (~100 keV/μm) with those of β particles (<1 keV/μm): approximately four traversals of the cellular nucleus by the former will result in cell death whereas several thousand traversals by the latter are required for the same result.

Specificity: The radionuclide must be delivered preferentially to the disease location with minimal uptake by normal tissues. This specificity is achieved through the choice of an appropriate vector. This can be simply the chemical form used. For example, radium chloride has a high uptake in bone and has

been used (with various isotopes of radium) for the treatment of ankylosing spondylitis, bone tuberculosis, and osseous metastases. Monoclonal antibodies can be labeled with particulate-emitting radionuclides.

Physical half-life: From Chap. 5, the effective half-life is a function of the physical half-life of the radioisotope used and the biological half-life of the labeled moiety in the targeted organ or tissue. Here, we shall presume that the letter is a component of the specificity category above and consider the former. We have seen how the biological effects of irradiation are a function of the rate at which the absorbed dose is delivered and the α/β ratio of the tissue in question. For radionuclide therapy, this effect is demonstrated by the Lea–Catcheside dose-protraction factor. Howell et al. (1994) used the LQ model to incorporate the rate of repair, the rate at which the absorbed dose is delivered, the physical and biological half-lives of the radioactive moiety and the required absorbed dose to conclude that radionuclides with longer half-lives were more advantageous in radionuclide therapy. They concluded that the optimal physical half-life of the radionuclide should be two to three times greater than the biological clearance half-life. For example, consider the effective half-life given by (5.10) in which the physical half-life is $T_{1/2,\mathrm{Phys}} = 3T_{1/2,\mathrm{Biol}}$. Then,

$$T_{1/2,\mathrm{eff}} = \frac{3}{2} T_{1/2,\mathrm{Phys}} \tag{10.53}$$

The authors concluded that among the β-emitting isotopes, ^{32}P, with a 14.126 day half-life, would be optimal for radionuclide therapy. Rao and Howell (1993) demonstrated how time-fractionation from external beam radiotherapy can offer guidance on selection of the radionuclide half-life.

Currently, most radionuclide therapy is based upon the use of β-emitting isotopes such as ^{131}I and ^{90}Y with maximum kinetic energies of 610 keV and 2.28 MeV, respectively. Hence, the associated LET values will be low, although the range of these β particles are several millimeter which could be advantageous if there is not a specific uptake of the isotopes into the nucleus of the target tumor cell. α-emitting isotopes are progressing into the radionuclide therapy field, examples being ^{211}At and ^{226}Ra. α particles exhibit high LET and the typical range of them are several cell diameters. Hence, α-emitting isotopes can be more efficient at producing lethal effects.

Auger/Coster–Kronig electrons are particularly advantageous in delivering a high absorbed dose to a small volume. Even ^{99m}Tc has an Auger/Coster–Kronig electron component, releasing, on average, four such electrons per decay and depositing nearly 300 eV within a 5 nm sphere around the nuclide. ^{125}I emits an average of 20 Auger/Coster–Kronig electrons per decay which deposit an energy of about 1 keV within a 5 nm sphere. The high-energy depositions in small volumes associated with Auger/Coster–Kronig emissions demonstrates that the short ranges of these electrons requires that the radionuclides to be incorporated within the cellular nucleus in order to be in close proximity to the DNA target (or even incorporated within it) in order to yield tumor cell inactivation.

References

Baechler S, Hobbs RF, Prideaux AR et al (2008) Extension of the biological effective dose to the MIRD schema and possible implications in radionuclide therapy dosimetry. Med Phys 35:1123–1133

Barendsen GW, Koot CJ, van Kersen GR, Bewley DK, Field SB, Parnell CJ (1966) The effect of oxygen on impairment of the proliferative capacity of human cells in culture by ionizing radiations of different LET. Int J Radiat Biol Relat Stud Phys Chem Med 10:317–327

Barendsen GW (1968) Responses of cultured cells, tumors, and normal tissues to radiation of different linear energy transfer. Curr Top Radiat Res Q 4:293–356

Berrington A, Darbcy SC, Weiss HA, Doll R (2001) 100 years of observation on British radiologists: mortality from cancer and other causes 1897–1997. Br J Radiol 74:507–519

Bithell JF, Stiller CA (1988) A new calculation of the carcinogenic risk of obstetric x-raying. Stat Med 7:857–864

Boice JD Jr, Day NE, Andersen LA, Brinton R, Brown NW, Choi EA et al (1985) Second cancers following radiation treatment for cervical cancer: an international collaboration among cancer registries. J Natl Cancer Inst 74:955–975

Brenner DJ, Hlatky LR, Hahnfeldt PJ et al (1998) The linear-quadratic model and most other common radiobiological models result in similar predictions of time-dose relationships. Radiat Res 150:83–91

Brenner DJ, Hall EJ (2007) Computed tomography – an increasing source of radiation exposure. N Engl J Med 357:2277–2284

Brenner DJ (2008) Effective dose: a flawed concept that could and should be replaced. Br J Radiol 81:521–523
Cameron JR (2002) Radiation increased the longevity of British radiologists. Br J Radiol 75:637–639
Chan WS, Ginsberg J (1999) Management of venous thromboembolism in pregnancy. In: Oudkerk M, van Beek EJR, ten Cate JW (eds) Pulmonary embolism. Blackwell Science, Berlin
Cornforth MU, Bedford JS (1987) A quantitative comparison of potentially-lethal damage repair and the rejoining of interphase chromosome breaks in low passage normal human fibroblasts. Radiat Res 111:385–405
Dale RG (1985) The application of the linear quadratic dose-effect equation to fractionated and protracted radiotherapy. Br J Radiol 58:515–528
Dale RD (1996) Dose-rate effects in targeted radiotherapy. Phys Med Biol 41:1871–1884
Dietze G, Harrison JD, Menzel HG (2009) Letter to the editor. Br J Radiol 82:348–351
Doll R, Barrington A, Dary SV (2005) Low mortality of British radiologists. Br J Radiol 78:1057–1058
Folkard M, Prise KM, Vojnovic B (2007) Status of charged particle microbeams for radiation biology. J Phys 58: 62–67
Fowler JF, Stern BL (1960) Dose-rate effects: some theoretical and practical considerations. Br J Radiol 33:389–395
Frankenberg-Schwager M (1989) Review of repair kinetics for DNA damage induced in eukaryotic cells in vitro by ionizing radiation. Radiother Oncol 14:307–320
Goodhead DT (1985) Saturable repair models of radiation action in mammalian cells. Radiat Res Suppl 104: S58–S67
Hall EJ (2003) The bystander effect. Health Phys 85:31–35
Hall EJ, Giaccia AJ (2006) Radiobiology for the radiologist, 6th edn. Lippincott, Williams & Wilkins, Philadelphia
Howell RW, Goddu SM, Rao DV (1994) Application of the linear-quadratic model to radioimmunotherapy: further support for the advantage of longer-lived radionuclides. J Nucl Med 35:1861–1869
ICRP (1959) Recommendations of the International Commission on Radiological Protection. ICRP Publication 1. Pergamon, Oxford
ICRP (1964) Recommendations of the International Commission on Radiological Protection. ICRP Publication 6. Pergamon, Oxford
ICRP (1966) Recommendations of the International Commission on Radiological Protection. ICRP Publication 9. Pergamon, Oxford
ICRP (1977) Recommendations of the International Commission on Radiological Protection. ICRP Publication 26. Pergamon, Oxford
ICRP (1991) Recommendations of the International Commission on Radiological Protection. ICRP Publication 60. Pergamon, Oxford
ICRP (2007) The 2007 Recommendations of the International Commission on Radiological Protection. ICRP Publication 103. Pergamon, Oxford
Kahim MA, Macdonal DA, Goodhead DT, Lorimore SA, Marsden SJ, Wright EG (1992) Transmission of chromosomal instability after plutonium α-particle irradiation. Nature 355:738–740
Kassis AI, Havell RW, Sastry KSR, Adelstein SJ (1988) Positional effects of Auger decays in mammalian cells in culture. In: Baverstock KF, Charlton DE (eds) DNA: damage by Auger emitters. Taylor and Francis, London
Kassis AI (2003) Radiobiology aspects and radionuclide selection criteria in cancer therapy. In: Zaidi H, Sgouros G (eds) Therapeutic applications of Monte Carlo calculations in nuclear medicine. Institute of Physics, Bristol
Kleinerman RA, Boice JD, Storm HH, Sparen P, Andersen A, Pukkala E, Lynch CF, Hankey BF, Flannery JT (1995) Second primary cancer after treatment for cervical cancer: an international cancer registries study. Cancer 76:442–452
Lea DE, Catcheside DG (1942) The mechanism of the induction by radiation of chromosome aberrations in Tradescantia. J Genet 44:216–245
Luckey TD (1991) Radiation hormesis. CRC, Boca Raton
McParland BJ (1990) The effect of a dynamic wedge in the medial tangential field upon the contralateral breast dose. Int J Radiat Oncol Biol Phys 19:1515–1520
McParland BJ, Fair HI (1992) A method of calculating peripheral dose distributions of photon beams below 10 MV. Med Phys 19:283–293
MacMahon B (1962) Prenatal X-ray exposure and childhood cancer. J Natl Cancer Inst 28:1173–1191
Martin CJ (2007) Effective dose: how should it be applied to medical exposures? Br J Radiol 80:639–647
Meredith R, Wessels B, Knox S (2008) Risks to normal tissues from radionuclide therapy. Semin Nucl Med 38:347–357
Mothersill C, Seymour C (2001) Radiation-induced bystander effects: past history and future directions. Radiat Res 155:759–767
Munro TR (1961) Irradiation of selected parts of single cells. Ann NY Acad Sci 95:920–931
Nagasawa H, Little JB (1992) Induction of sister chromatid exchanges by extremely low doses of α-particles. Cancer Res 52:6394–6396
Nais AHW (1998) An introduction to radiobiology, 2nd edn. Wiley, Chichester
National Research Council (1990) Health effects of exposure to low levels of ionizing radiation BEIR V. National Academy Press, Washington, DC
National Research Council (2006) Health effects of exposure to low levels of ionizing radiation BEIR VII Phase 2. National Academy Press, Washington, DC
Radiation Effects Research Foundation (1987a) US-Japan joint reassessment of atomic bomb radiation dosimetry in Hiroshima and Nagasaki – final report, vol 1. Radiation Effects Research Foundation, Hiroshima
Radiation Effects Research Foundation (1987b) US-Japan joint reassessment of atomic bomb radiation dosimetry in Hiroshima and Nagasaki – final Report, vol 2. Radiation Effects Research Foundation, Hiroshima
Rao DV, Howell RW (1993) Time-dose-fractionation in radioimmunotherapy: implications for selecting radionuclides. J Nucl Med 34:1801–1810
Ron E, Modan B, Boice JD Jr (1988) Mortality after radiotherapy for ringworm of the scalp. Am J Epidemiol 127: 713–725
Ron E (1998) Ionizing radiation and cancer risk: evidence from epidemiology. Radiat Res 150:S30–S41

Russell LB, Russell WL (1954) An analysis of the changing radiation response of the developing mouse embryo. J Cell Physiol 43(S1):130–149

Sachs RK, Hahnfield P, Brenner DJ (1997) The link between low-LET dose-response relations and the underlying kinetics of damage production/repair/misrepair. Int J Radiat Biol 72:351–374

Savage JRK (1983) Some practical notes on chromosomal aberrations. Clin Cytogen Bull 1:64–76

Sgouros G, Knowx SJ, Joiner MC et al (2007) IRD continuing education: bystander and low-dose-rate effects: are these relevant to radionuclide therapy? J Nucl Med 48:1683–1691

Shore RE, Albert RE, Pasternack BS (1976) Follow-up study of patients treated by X-ray epilation for tinea capitis: re-survey of post-treatment illness and mortality experience. Arch Environ Health 31:17–24

Stewart A, Webb J, Giles D, Hewitt D (1956) Malignant disease in childhood and diagnostic irradiation in utero. Lancet 271 (6940):447–448

Stewart A, Webb J, Hewitt D (1958) A survey of childhood malignancies. Br Med J 1:1495–1508

Stovall M, Blackwell R, Cundiff J et al (1995) Fetal dose from radiotherapy with photon beams. Med Phys 22:63–82

Weiss HA, Darby SC, Doll R (1994) Cancer mortality following x-ray treatment for ankylosing spondylitis. Int J Cancer 59:327–338

Wessels BW, Konijnenberg MW, Dale RG, Breitz HB, Cremonesi M, Meredith RF et al (2008) MIRD Pamphlet No. 20: the effect of model assumptions on kidney dosimetry and response – implications for radionuclide therapy. J Nucl Med 49:1884–1899

Wheldon TE, O'Donoghue JA (1990) The radiobiology of targeted radiotherapy. Int J Radiat Biol 59:1–21